

December 2018

CFD Modeling of Smoke Movement in an Atrium

Robin Wu
rlwu@crimson.ua.edu

Follow this and additional works at: <https://digitalscholarship.unlv.edu/thesesdissertations>



Part of the [Aerodynamics and Fluid Mechanics Commons](#), [Mechanical Engineering Commons](#), and the [Thermodynamics Commons](#)

Repository Citation

Wu, Robin, "CFD Modeling of Smoke Movement in an Atrium" (2018). *UNLV Theses, Dissertations, Professional Papers, and Capstones*. 3535.

<https://digitalscholarship.unlv.edu/thesesdissertations/3535>

This Thesis is protected by copyright and/or related rights. It has been brought to you by Digital Scholarship@UNLV with permission from the rights-holder(s). You are free to use this Thesis in any way that is permitted by the copyright and related rights legislation that applies to your use. For other uses you need to obtain permission from the rights-holder(s) directly, unless additional rights are indicated by a Creative Commons license in the record and/or on the work itself.

This Thesis has been accepted for inclusion in UNLV Theses, Dissertations, Professional Papers, and Capstones by an authorized administrator of Digital Scholarship@UNLV. For more information, please contact digitalscholarship@unlv.edu.

CFD MODELING OF SMOKE MOVEMENT IN AN ATRIUM

by

Robin L. Wu

Bachelor of Science - Chemical and Biological Engineering
The University of Alabama
2012

A thesis submitted in partial fulfillment
of the requirements of the

Master of Science in Engineering - Mechanical Engineering

Department of Mechanical Engineering
Howard R. Hughes College of Engineering
The Graduate College

University of Nevada, Las Vegas
December 2018

Copyright 2018 by Robin Wu

All Rights Reserved



Thesis Approval

The Graduate College
The University of Nevada, Las Vegas

September 24, 2018

This thesis prepared by

Robin L. Wu

entitled

CFD Simulation of Smoke Movement in an Atrium

is approved in partial fulfillment of the requirements for the degree of

Master of Science in Engineering - Mechanical Engineering
Department of Mechanical Engineering

Samir Moujaes, Ph.D.
Examination Committee Chair

Kathryn Hausbeck Korgan, Ph.D.
Graduate College Interim Dean

Alexander Barzilov, Ph.D.
Examination Committee Member

Hui Zhao, Ph.D.
Examination Committee Member

Samaan Ladkany, Ph.D.
Graduate College Faculty Representative

Abstract

The purpose of this paper is to better understand the behavior of smoke movement in an atrium. Thus gives first responders and civilians in and out of building a better understanding of best ways to save lives and to minimize losses due to fire or smoke damages.

With the advancements of modern technology, computers and softwares make simulation models possible such as fire models to simulate fire and smoke movements. In this paper, a computational fluid dynamic (CFD) software Fire Dynamic Simulator (FDS) is used to conduct a series of atrium tests to investigate the effectiveness of smoke exhaust systems. FDS solves the Navier-Stokes equations appropriate for low speed flows ($Ma < 0.3$) with an emphasis on smoke, heat transport and CO_2 concentrations from fires. The default turbulence model used in FDS simulation is the Large Eddy Simulation (LES), which is the solution of Navier-Stokes equations at low speed.

The compartment tested was $9\text{ m} \times 6\text{ m} \times 5.5\text{ m}$ height which is the same conditions used in Hadjisophocleous, Fu, and Lougheed [6]. In their paper, the measured exhaust rates used ranged from 2.0 to 5.0 kg/s with thermocouples placed at various heights to see the upper smoke layer and the lower air layer along with the convective boundary layer or interface layer. CO_2 concentrations, heat release rates, and temperatures are looked at to better understand the behavior of smoke. Keep in mind that this is only a short term test of 1300 seconds of simulations time. Also note that FDS does not simulate the burning of materials. There are other softwares like CFAST and PyroSim would better support this. FDS also does not consider flashovers.

FDS applies Deardorff's turbulence model [3] and Smagorinsky model [14] to predict the CO_2 concentration, upper smoke layer and temperatures. Both these models are briefly described in this paper with focus on fluid flow at low speeds. The results from the model

are compared to the experimental results by Hadjisophocleous, Fu, and Lougheed [6] to see if the CO₂ concentrations and heat release rates are similar.

Acknowledgements

I would like to sincerely thank my advisor Dr. Moujaes for his continuous guidance, support and encouragement of my academic endeavors. His enthusiasm, motivation, and immense knowledge has guided me in my graduate experiences from thesis topic to research to writing my thesis. It couldn't imagine a different mentor and advisor for my master's study.

Dr. Barzilov, Dr. Ladkany, and Dr. Zhao thank you for being on my committee and for all the encouragement, insightful comments, and tough questions.

Lastly I would like to thank my family: my parents for supporting me financially and spiritually throughout my life and my brother for his support and encouragement. I would also like to thank my fiancée in her understanding and support.

Contents

Abstract	iii
Acknowledgements	v
List of Tables	viii
List of Figures	ix
List of Equations	xii
Chapter 1. Introduction	1
1.1. Background	1
1.2. Simple Mathematical Models	3
1.3. Other Models	5
Chapter 2. Material and Methods	9
2.1. Deardorff Model	10
2.2. Smagorinsky Model	11
2.3. Heat Transfer Model	11
Chapter 3. Simulation Model	13
3.1. Hardware	16
3.2. Grid Independence	17
Chapter 4. Results and Comparisons	21
4.1. CO ₂ Concentration results	21
4.2. Temperatures at various heights.	25
4.3. Heat release rates at various fire sizes.	37
4.4. Temperature and Velocity Fields	39
Chapter 5. Final Remark	49

Appendix A. FDS Code for this thesis	51
Bibliography	56
Curriculum Vitae	58

List of Tables

2.1	Thermal Properties	9
2.2	Dimensions	9
3.1	Simulation Settings	16
3.2	Grid Independence	19

List of Figures

3.1	Original model	13
3.2	FDS model in simulation	14
3.3	View from below	14
3.4	Simulation time vs CPU time	16
3.5	Grid Independence	17
3.6	Relative Error	18
3.7	Relative Error	20
4.1	CO ₂ concentration results from [6]	22
4.2	CO ₂ concentration results produced by FDS	22
4.3	Simulated results in blue vs [6]	24
4.4	Simulated results in blue (shifted right) versus [6]	24
4.5	Exhaust vent: 3 - 4 m ³ /s, thermocouples at 1m, cor=0.656682	26
4.6	Exhaust vent: 3 - 4 m ³ /s, thermocouples at 2m, cor=0.655044	26
4.7	Exhaust vent: 3 - 4 m ³ /s, thermocouples at 3m, cor=0.655044	27
4.8	Exhaust vent: 3 - 4 m ³ /s, thermocouples at 4m, cor=0.831521	27
4.9	Exhaust vent: 3 - 4 m ³ /s, thermocouples at 5m, cor=0.799095	28
4.10	Exhaust vent: 3 - 4 m ³ /s, thermocouples at 1m, cor=0.736384	28
4.11	Exhaust vent: 3 - 4 m ³ /s, thermocouples at 2m, cor=0.846941	29
4.12	Exhaust vent: 3 - 4 m ³ /s, thermocouples at 3m, cor=0.884347	29
4.13	Exhaust vent: 3 - 4 m ³ /s, thermocouples at 4m, cor=0.858694	30
4.14	Exhaust vent: 3 - 4 m ³ /s, thermocouples at 5m, cor=0.82056	30
4.15	Exhaust vent: 3 - 4 m ³ /s, thermocouples at 1m, cor=0.668855	31
4.16	Exhaust vent: 3 - 4 m ³ /s, thermocouples at 2m, cor=0.792164	31

4.17 Exhaust vent: 3 - 4 m ³ /s, thermocouples at 3m, cor=0.914492	32
4.18 Exhaust vent: 3 - 4 m ³ /s, thermocouples at 4m, cor=0.876691	32
4.19 Exhaust vent: 3 - 4 m ³ /s, thermocouples at 5m, cor=0.840092	33
4.20 Exhaust vent: 3 m ³ /s. Thermocouples at 1 - 5m high	33
4.21 Exhaust vent: 4 m ³ /s. Thermocouples at 1 - 5m high	34
4.22 Exhaust vent: 3 m ³ /s. Thermocouples at 1 - 5m high	34
4.23 Exhaust vent: 4 m ³ /s. Thermocouples at 1 - 5m high	35
4.24 Exhaust vent: 3 m ³ /s. Thermocouples at 1 - 5m high	35
4.25 Exhaust vent: 4 m ³ /s. Thermocouples at 1 - 5m high	36
4.26 Heat release rate at 150kW	37
4.27 Heat release rate at 300kW	38
4.28 Heat release rate at 600kW	38
4.29 Temperature field in the z-plane	39
4.30 Temperature field in the z-plane	40
4.31 Temperature field in the z-plane	40
4.32 Temperature field in the y-plane	41
4.33 Temperature field in the z-plane	41
4.34 Temperature field in the z-plane	42
4.35 Temperature field in the x-plane	42
4.36 Temperature field in the y-plane	43
4.37 Velocity field in the z-plane	45
4.38 Velocity field in the z-plane	46
4.39 Velocity field in the z-plane	46
4.40 Velocity field in the y-plane	47

4.41	Velocity field in the y -plane	47
4.42	Velocity field in the z -plane	48

List of Equations

Eq (1.2.1)	3
Eq (1.2.2)	3
Eq (1.2.3)	4
Eq (1.2.4)	4
Eq (1.2.5)	4
Eq (1.2.6)	4
Eq (1.2.7)	4
Eq (1.2.8)	5
Eq (1.2.9)	5
Eq (1.2.10)	5
Eq (1.3.1)	6
Eq (1.3.2)	6
Eq (1.3.3)	7
Eq (1.3.4)	7
Eq (1.3.5)	7
Eq (1.3.6)	7
Eq (1.3.7)	7
Eq (2.1.1)	10
Eq (2.2.1)	11
Eq (2.2.2)	11
Eq (2.3.1)	11
Eq (2.3.2)	12
Eq (4.1.1)	23

CHAPTER 1

INTRODUCTION

1.1. Background

According to Wikipedia [19], some 50% to 80% of all fire related deaths are from smoke inhalation. Victims are killed by a variation of thermal damage, poisoning, pulmonary irritation and swelling caused by many combustible products. According to U.S. Fire Administration [4] in 2016, 3,515 lives were taken due to fire. That means some 1,758 to 2,812 people were killed due to smoke inhalation. This should be a strong reason, why more focus on the behavior of smoke should be investigated, in order to save more lives when a fire breaks out or possibly lowering the percentage of victims who die from smoke inhalation.

In the Hadjisophocleous, Fu, and Lougheed [6] the effectiveness of smoke exhaust systems with ranges of 1.94 kg/s to 5.13 kg/s were tested in atriums. The atrium dimensions used was $9\text{ m} \times 6\text{ m} \times 5.5\text{ m}$ height with heat release rates ranging from 15 kW to 1000 kW. The paper analyzes large undivided spaces known as atriums within buildings. When a fire breaks out the smoke is known to spread to connecting rooms which endangers the occupants in the building. The purpose of a smart smoke management systems is to limit the spread of smoke from one space to other connecting rooms or areas and to allow the escape of occupants. To achieve this, smoke has to be confined to limited areas. This in turn limits the toxic gases, limits the smoke layer temperature, and allows for a unclouded height at certain levels for a finite amount of time.

Fire Dynamic Simulator (FDS) was first released to the public in February 2000 [11]. Throughout the development, FDS was designed to solve practical fire problems while also providing tools to study fundamental fire dynamic and combustion. Roughly, half of the

applications to date are designed for smoke handling systems, detectors and sprinkler activation studies. The other half is consisted of the reconstruction of residential and industrial fires.

FDS numerically solves Navier-Stokes equation at low speed conditions and thermally-driven flow, with Large Eddy Simulation (LES) as the default mode of operation.

Hydrodynamic Model: Two surface models are applied for the radiative heat transfer. The radiation flux is assumed to be uniform for the assumed sphere for the flame.

Combustion Model: FDS is able to uses single step and mix controlled chemical reactions. This uses a three lumped species method, a species is represented by grouping of species, they are fuel, air, and products.

Radiation Transport: The radiative heat transfer equation is solved using techniques similar to finite volume methods for convective transport which uses roughly 100 discrete angles. The finite volume solver within FDS requires 20% of total CPU time. FDS uses RadCal narrow band model to compute the absorption coefficients of gas and soot mixtures [11] with liquid droplets that can scatter and absorb thermal radiation.

Geometry: FDS uses rectilinear mesh to approximate the governing equations. Which allows rectangular obstructions to conform with the underlying mesh.

Multiple Mesh: FDS allows the use of multiple rectangular mesh in a calculation.

Parallel Processing: FDS uses programming interface which allows multiple processing units on a single computer.

Boundary Conditions: All solid surfaces have thermal boundary conditions and burning the behavior of most materials. The heat transfer to and from solid surfaces are based on empirical correlations.

1.2. Simple Mathematical Models

To describe fluid flow, heat transfer, and radiation Partial differential equations (PDEs) can be useful. Such a mathematical model usually consists of a group of PDEs attached with certain initial and boundary conditions. The solution of such a model provides a key to understand the dynamics. Thus the computer simulations based on the solutions (numerical) of such models are of great importance.

Temperature distributions, like air flow, can be modeled by Navier-Stokes Equations (NSE) attached with a heat transfer equation. Many researchers agree that this approach is highly accurate and successful, however it requires heavy computational effort due to the nonlinearity of NSE.

To have a taste of mathematical models, let's consider a simple model of air flow and assume that the flow is incompressible and irrotational, that is the constant air density ρ and a zero of the Curl of the air velocity field. We also want to neglect the effects of air viscosity and turbulence for simplicity.

Denote by

$$\nabla = \left(\frac{\partial}{\partial x}, \frac{\partial}{\partial y}, \frac{\partial}{\partial z} \right) \quad \text{and} \quad \Delta = \nabla^2 = \frac{\partial^2}{\partial x^2} + \frac{\partial^2}{\partial y^2} + \frac{\partial^2}{\partial z^2}. \quad (1.2.1)$$

Let v be the velocity field for air. The equations

$$\nabla \cdot v = 0 \quad \text{and} \quad \nabla \times v = 0 \quad (1.2.2)$$

are the consequences of the two assumptions, incompressibility and the irrotational, respectively. From Calculus, we know that the velocity field v must be the gradient of a scalar function φ , that is

$$v = \nabla\varphi \tag{1.2.3}$$

Such a function φ is known as a potential of the velocity field v . Applying the mass transport equation

$$\frac{\partial\rho}{\partial t} + \nabla \cdot (\rho v) = 0 \tag{1.2.4}$$

and using the assumption $\rho = \text{constant}$ (ρ is the air density), we obtain the simplified mass transport equation $\nabla \cdot (\rho \nabla\varphi) = 0$, which is the Laplace equation

$$\Delta\varphi = 0 \tag{1.2.5}$$

To represent the situation where the sinks and sources of a fluid are located on the boundaries of the domain, we can use the Neumann boundary condition,

$$n \cdot \nabla\varphi = v_N \tag{1.2.6}$$

where n is the outward unit normal vector on the boundary of the domain and v_N is a function representing the boundary value of air velocity at boundary of the domain. Other boundaries, such as walls, have a no slip condition, that is $v_N = 0$.

It is clear that the solutions to the above boundary value problems may differ by a constant. The solution will be unique when a Dirichlet boundary condition is added:

$$\varphi = \varphi_D \tag{1.2.7}$$

where φ_D is the desired boundary value for the the potential function on the boundary of the domain.

To model a steady-state temperature distribution and the heat transfer, we can use the convection-diffusion equation

$$\rho C_p v \cdot \nabla T - \nabla \cdot (k \nabla T) = 0, \quad (1.2.8)$$

where T is the temperature, ρ , c_p and k are the density, specific heat and thermal conductivity of air, respectively.

As before, the above model should be assigned with an appropriate boundary conditions on temperature and/or heat flow at the boundary of the domain. Naturally, this should be the Dirichlet boundary condition

$$T = T_D \quad (1.2.9)$$

where T_D is the function representing the value of T at the boundary of the domain.

The heat flow normal to the boundary of the domain can be described by the Neumann condition

$$-n \cdot (k \nabla T) = q. \quad (1.2.10)$$

Above presented models are just simple models good for some simple cases, and they do not suit for all cases. Many times each case requires its own specific model to obtain the most practical and realistic results.

1.3. Other Models

Combustion and Chemistry

The combustion from fuel to fire is calculated by the fuel to oxygen ratio. There must be sufficient oxygen for the fire plume to be realistic. FDS uses a three lumped species, which are air, fuel and product. The chemistry mass ratio with respect to fuel and carbon related products are carbon dioxide, carbon monoxide, and soot.

Heat Transfer

Convection and radiation are two types of heat transfer that need to be considered. The convection through compartments and other surfaces in the fire rooms along with the rooms without fires is considered to be natural convection for FDS [8] and its default model for this simulation.

Fluid Flow Model

Two types of models are applied, one is the McCaffrey's [10] and the Heskestad's model [7].

$$\frac{\dot{m}_e}{Q_c} = C_{e1} \left(\frac{Z_e}{Q_c^{0.4}} \right)^{C_{e2}} \quad (1.3.1)$$

where

Q_c = convective heat release rate,

\dot{m}_e = mass entrainment rate,

Z_e = plume entrainment height,

C_{e1} and C_{e2} = constant coefficients.

for McCaffrey's model and for Heskestad's model, if

$$\frac{Z_e}{Q_c^{0.4}} \leq 0.166, \quad \frac{\dot{m}_e}{Q_c} = 0.034 \frac{Z_e}{Q_c^{0.4}} \quad (1.3.2)$$

if

$$\frac{Z_e}{Q_c^{0.4}} > 0.166, \quad \frac{\dot{m}_e}{Q_c} = 0.071 \left(\frac{Z_e}{Q_c^{0.4}} \right)^{\text{ceil}^5} + 0.0018 \quad (1.3.3)$$

Mechanical Ventilation

Mechanical ventilation mechanism is applied so that smoke can be extracted and air can be supplied. The vertical extension of the opening and the volume or mass flow rate of the ventilation are the two parameters that are specified. Initially, when a fire breaks out the smoke rises to the ceiling. Thus causing two layers one of smoke at the top and the lower layer is air. When the plume entrainment rate is greater than that of the exhaust rate, the exhausted gas will only be smoke. If the exhaust rate is higher than the smoke entrainment rate, the smoke exhaust system is said to be ideally effective. For this mass flow rate and volume flow rate specification are considered.

$$\dot{m}_{MU} = \min(\dot{m}_{Fan}, \dot{m}_{max}) \quad (1.3.4)$$

$$\dot{m}_{ML} = \dot{m}_{Fan} - \dot{m}_{max} \quad (1.3.5)$$

and

$$\dot{V}_{MU} = \min(\dot{V}_{Fan}, \frac{\dot{m}_{max}}{\rho_U}) \quad (1.3.6)$$

$$\dot{V}_{ML} = \dot{V}_{Fan} - \dot{V}_{MU} \quad (1.3.7)$$

Where \dot{m}_{max} is the max smoke exhaust vent rate for the upper layer. \dot{m}_{MU} and \dot{m}_{ML} are the mass flow rate exhausted for the upper and the lower layers, respectively. The \dot{m}_{Fan} is the mass exhaust rate of the exhaust vent. \dot{V}_{MU} and \dot{V}_{ML} is the volume flow rate exhaust

for the upper and lower layer. \dot{V}_{Fan} is the volume exhaust rate from the exhaust vent. ρ_U is the density of the smoke layer. It is difficult to calculate \dot{m}_{max} sometimes it needs to be set as the plume entrainment rate so that a small distance beneath the opening will keep the smoke interface below the opening.

CHAPTER 2

MATERIAL AND METHODS

FDS is a computational fluid dynamic model for fluid flow driven by fire. The numerical solver is designed for low speed fluid flow or Mach numbers less than 0.3 with the appropriate Navier-Stokes equations. FDS takes in to consideration of smoke and heat transport from fires and the heat release rate (HRR) of the fire. Each compartment in the floor plan connected by a door leading into each of the compartments with ceiling vents in every compartment. CO₂ inlet is placed in a room to help with finding the comparable results in the experimental model to the simulation model.

TABLE 2.1. **Thermal Properties**

	Ceiling	Walls	Floors
Thickness-(m)	0.025	0.025	0.025
Density-(kg m ⁻³)	130	130	130
Conductivity-(W m ⁻¹ K ⁻¹)	0.08	0.08	0.08
Specific Heat-(J kg ⁻¹ K ⁻¹)	900	900	900
Surface Emissivity	0.9	0.9	0.9

TABLE 2.2. **Dimensions**

	Length	Width	Height
Compartment (m)	9	6	5.5
Floor Vent (m)	22.8	0.1	-
Burner's Surface (m)	4.5	3	0.2

2.1. Deardorff Model

FDS by default, uses Deardorff for turbulent viscosity which is a three-dimensional model. This model was also used to model stratocumulus clouds, which is also very similar to smoke.

$$\mu_t = \rho C_v \Delta \sqrt{k_{sgs}} ; k_{sgs} = \frac{1}{2} ((\bar{u} - \hat{u})^2 + (\bar{v} - \hat{v})^2 + (\bar{w} - \hat{w})^2) \quad (2.1.1)$$

where \bar{u} is the average value of the u grid cell center and \hat{u} is the weighted average of u over the adjacent cells.

The Deardorff model [3][12] is a three-dimensional model used to analyze turbulence and entrainment within stratocumulus clouds. This is to better understand the turbulent interaction between the capping inversion and the convective boundary layer. This is similar to smoke in a building creating a lower air layer with an upper layer of smoke. The major assumptions for the model includes the base of the capping inversion has a well mixed or uniform boundary layer, negligible thickness of the capping inversion, no holes of unsaturated air in the saturated part of the upper cloudy portion of the mixed layer and the buoyancy flux of entrainment occurs in saturated air, while none of the vertical mixing is due to wind shear but rather from buoyancy forces, no drizzle or precipitation, the divergence from net irradiance does not all occur within the upper mixed layer but occurs within the capping inversion, and the jump in equivalent potential temperature or wet-bulb potential temperature must be positive across the capping inversion for parcel stability.

2.2. Smagorinsky Model

The Smagorinsky model [15][12] is used due to the ill-defined off-wall grid cell which the Deardorff model does not. To achieve the no slip condition, FDS applies the damping function to the eddy viscosity so that it goes to zero as you approach the wall.

$$\bar{u}_{ijk} = \frac{u_{ijk} + u_{i-1,jk}}{2} ; \quad \hat{u}_{ijk} = \frac{\bar{u}_{ijk}}{2} + \frac{\bar{u}_{i-1,jk} + \bar{u}_{i+1,jk}}{4} \quad (2.2.1)$$

The terms \hat{v} and \hat{w} are defined similarly. Where $C_v = 0.1$ and $\Delta = (\delta x \delta y \delta z)^{(1/3)}$ which is the LES filter width taken from the geometric mean of the local mesh spacing in each direction. The turbulent viscosity also is related to the thermal conductivity and material diffusivity which are,

$$k_{LES} = \frac{\mu_{LES} C_p}{Pr_t} ; \quad (\rho D)_{LES} = \frac{\mu_{LES}}{Sc_t} \quad (2.2.2)$$

Here Pr_t the turbulent Prandtl number and Sc_t the Schmidt number is assumed to be 0.5 and 0.5 respectively for a given scenario.

2.3. Heat Transfer Model

The default heat transfer model [11][12] in the LES calculation is based on a combination of natural and forced convection correlation.

$$\dot{q}_c'' = h(T_g - T_w) \quad ; \quad h = \max \left[C \left| T_g - T_w \right|^{\frac{1}{3}} , \frac{k}{L} Nu , \frac{k}{\delta n} \right] \quad (2.3.1)$$

where \dot{q}_c'' is radiative heat, h is the convective heat transfer coefficient, Nu is the Nusselt number with depends on the geometry and flow characteristics. T_w is the surface temperature and T_g is the gas temperature. The other main heat transfer model used is the direct

numerical simulation (DNS) [11][12] which FDS uses this model to compute the velocity gradient at the wall from the resolved velocity near the wall.

$$\dot{q}_c'' = -k \frac{\partial T}{\partial n} = -k \frac{T_w - T_g}{\delta n/2} \quad (2.3.2)$$

where k is thermal conductivity of gas used, n is spatial coordinate pointing into a solid, and δn is normal grid spacing.

CHAPTER 3

SIMULATION MODEL

A diagram of the experimental facility is provided in the following. A simulation model was built based on Hadjisophocleous, Fu, and Lougheed [6] original model.

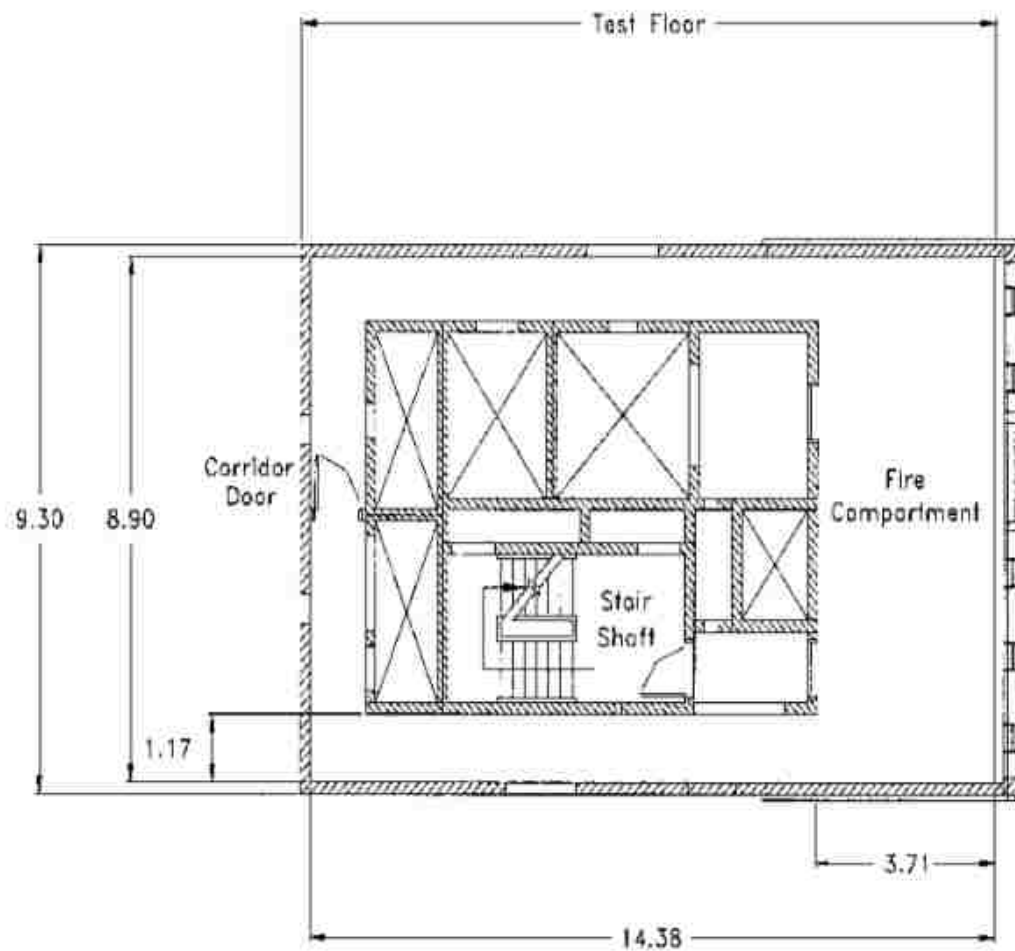


FIGURE 3.1. Original model

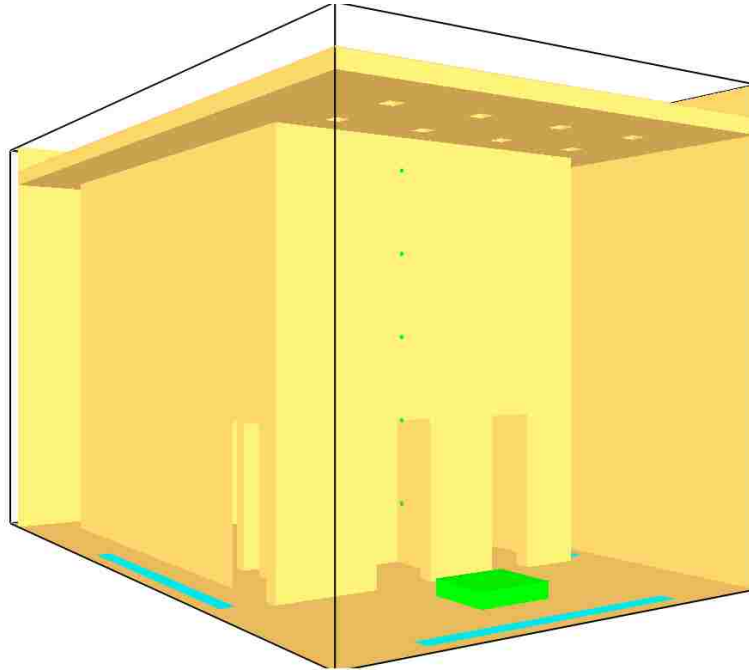


FIGURE 3.2. FDS model in simulation

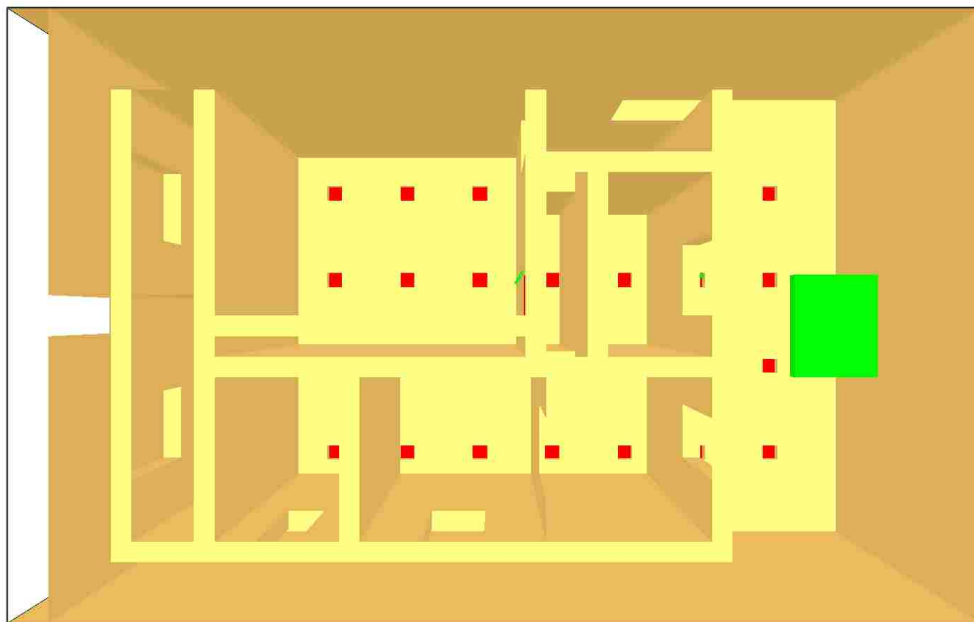


FIGURE 3.3. View from below

The facility is 9 m by 6 m by 5.5 m height in dimensions. From line 3 in Appendix A the meshing and the size of the model is defined starting with the x-axis to the z-axis.

In Figure 3.3, the red squares are exhaust vents on the ceiling and the green rectangle on the floor is the propane burner. In Figure 3.2 the cyan colored strips on the ground are floor vents that pulls fresh air from the outside. The little green dots in Figure 3.2 to the left of the propane burner are thermocouples. 5 thermocouples are place 1 meter apart vertically. This is found in lines 36 through 48.

The interior walls of the compartment are insulated with 25 mm thick rock fiber insulation. Lines 11 to 19 define the material's properties. These properties can be edited at will. But the properties set are in correspondence to the experimental model. The interior walls are found in lines 54 to 77.

The compartment is also equipped with vents to provide outside air into the compartment from the openings in the floor, which have the dimensions of 0.1 m and a total length of 22.8 m. The openings in the floor are on all four side of the compartment. The floor vents are defined in lines 94 through 101. The compartment also contains 32 exhaust inlets, all with a diameter of 150 mm which are located on the ceiling of the compartment. The inlets will be used to extract the hot gases along with soot produced by the fire. The exhaust system has 2 different fan speeds to extract hot gasses at $3 \text{ m}^3/\text{s}$ and $4 \text{ m}^3/\text{s}$. This is found in lines 106 to 110. The "MULT" allows for objects, holes, and vents to be repeated over and over in a file. A propane burner is used as the fire source.

During the simulation, the burner simulated fires from ranges of 150 kW to 600 kW. Found in lines 9 and 10. HRRPUA is the heat release rate per unit area thus for aesthetics line 9 of the appendix HRRPUA is set to 600. We see the actual value is the desired heat release rate divided by the surface area of the propane burner. In line 51 of the appendix for aesthetics the dimension of the propane burner was set to 1 meter by 1 meter. Thermocouples are placed at different heights and located in one of the rooms to get temperature measurements and heat release rates of the fire.

3.1. Hardware

The hardware used to run the FDS simulations has the specifications 4 CPUs, 1.80 GHz, 32 GB RAM. To run $\sim 43,000$ nodes, it took 37,450 seconds (~ 31.2 hours of CPU time) to simulate 1300 seconds.

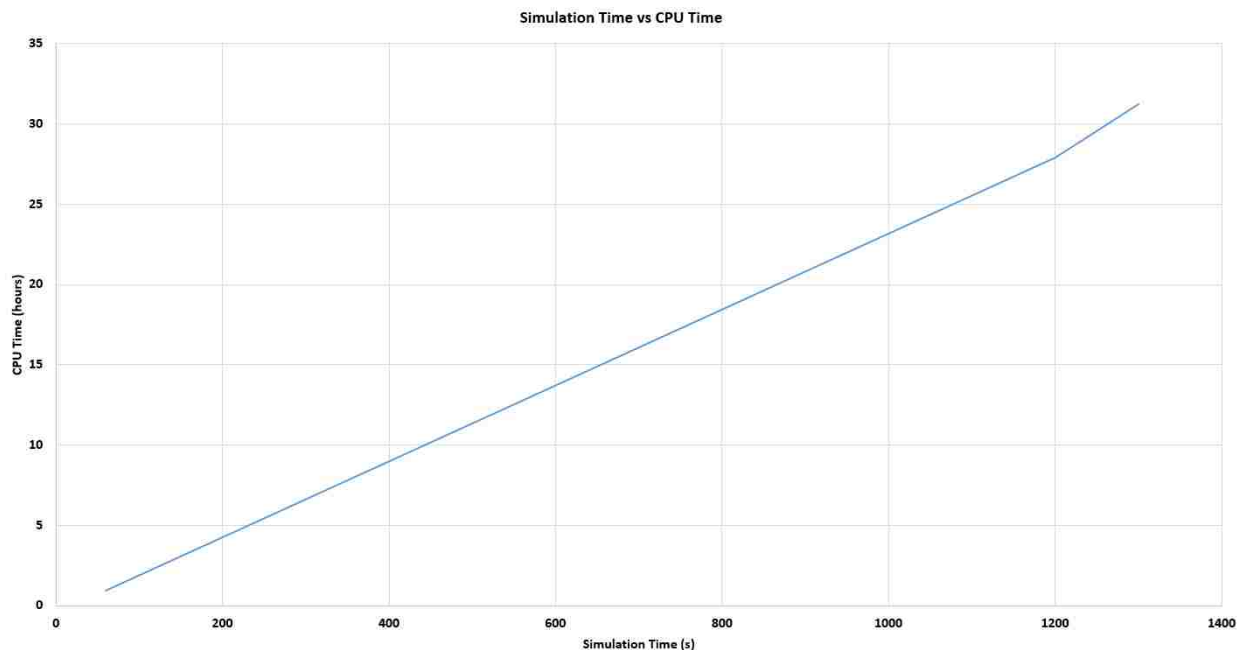


FIGURE 3.4. Simulation time vs CPU time

TABLE 3.1. Simulation Settings

Fire Sizes (kW)	150	300	600
Exhaust Vents (m^3/s)	3	4	
Floor Vents (m/s)	1.75		

3.2. Grid Independence

The simulation ran with atrium was done in 2 different node sizes. The first time was done with $\sim 43,000$ nodes. This took over 31 hours of CPU time. The second run was done with $\sim 342,000$ nodes which took over 150 hours of CPU time.

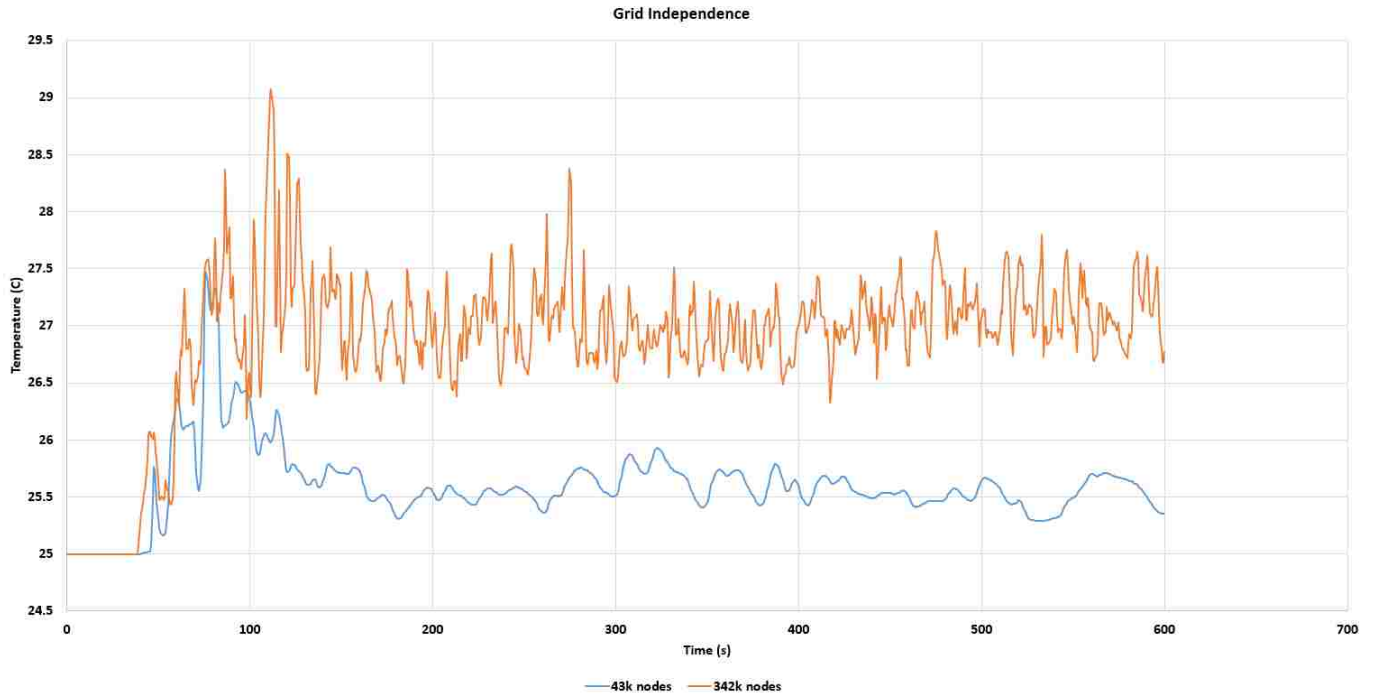


FIGURE 3.5. Grid Independence

The figure above shows two simulation runs (temperatures) under the exact same conditions with the exception of grid size. One with eight times more grids than the other. We see an obvious difference in temperatures and a lot more detail in the temperature read outs for the higher grid size. This shows grid size dependence. We also see a general similarity in the increases and decreases between the two graphs, which shows grid independence.

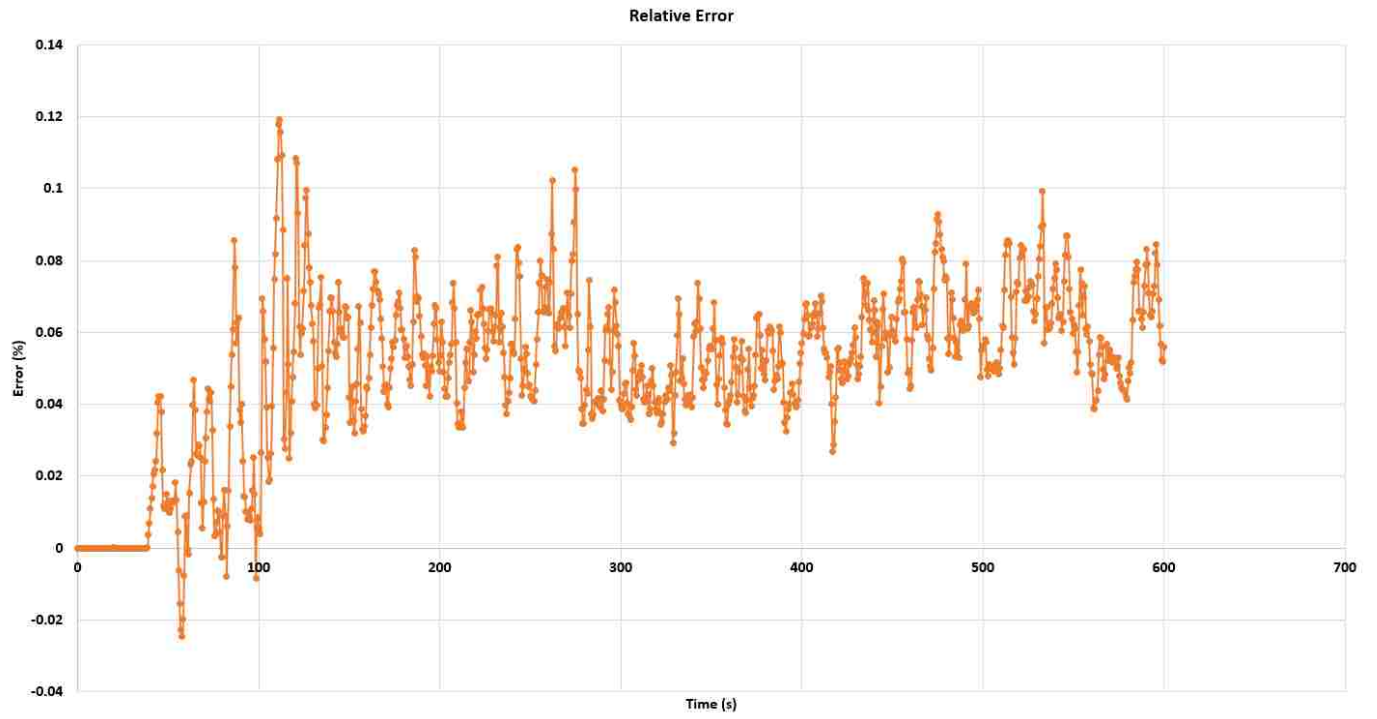


FIGURE 3.6. Relative Error

TABLE 3.2. Grid Independence

	Low Grid		Vs		High Grid	
	<i>Temp 1</i>	<i>Temp 3</i>	<i>Temp 5</i>	<i>Temp 1</i>	<i>Temp 3</i>	<i>Temp 5</i>
Initial values	25	25	25	25	25	25
	24.99995	24.9999	24.99992	24.99993	24.99992	24.99994
	24.99979	24.99964	24.9997	24.99975	24.99973	24.99972
	25.00059	24.99923	24.99936	25.00002	24.99939	24.99935
	25.00204	25.00489	24.999	25.00222	25.28138	24.99869
	25.00707	29.58132	24.99807	25.00232	57.716	27.05934
	25.1009	32.07081	64.8216	25.00184	27.33683	66.71692
	25.40584	25.52857	105.1287	25.00193	27.69437	121.6679
	25.19578	25.14257	94.77573	25.00294	36.41226	111.4933
	25.13967	25.46012	106.7275	25.00408	37.85887	109.3066
Final values	38.11955	177.7576	186.3002	35.56565	155.4223	218.662
	40.03196	176.6138	175.5376	40.92419	131.4096	217.1819
	43.33124	157.5448	190.0935	35.13093	150.9097	236.1302
	40.00769	195.1845	175.5492	35.96378	155.8507	283.5145
	61.70047	171.5539	189.8239	32.83527	199.0099	180.3324
	49.81982	147.8449	211.1205	33.60305	161.9698	178.7464
	47.31364	141.7112	169.5179	34.64841	141.0072	233.9655
	59.85478	160.0816	168.0128	34.78839	159.7724	212.4737
	46.1241	222.8105	171.4801	32.6528	160.7176	223.5819
	46.02894	169.4479	225.2386	31.23644	164.7835	193.3581



FIGURE 3.7. Relative Error

There are over one thousand data points for each column of temperature value in the table above. Only ten values from the initial and final points are listed in the table above.

Figure 3.5 compares graphically Temp 1 under low and high grids (from the table above). We do not feel its necessary to compare the other Temps.

CHAPTER 4

RESULTS AND COMPARISONS

4.1. CO₂ Concentration results

The experimental model done by Hadjisophocleous, Fu, and Lougheed [6] was very innovative, coming up with the idea to inject CO₂ in to the building to see if the interface height changed. This does not occur naturally during fires. Yes, a limited amount of CO₂ is produced from all the materials burned but nothing high enough to increase CO₂ concentration to 100%. With the results from the experimental model, an FDS simulation of the experimental model was done to verify the accuracy of FDS. Thus, a simulation of the experimental model was done with CO₂ injections. The results were very comparable to Hadjisophocleous, Fu, and Lougheed [6] from Figure 4.3.

The CO₂ concentration results in Figure 4.2 is comparable to the results in Figure 4.1 by the experimental model done by Hadjisophocleous, Fu, and Lougheed [6]. Minor differences are demonstrated in Figures 4.3 and 4.4. The computed rate of change of CO₂ concentration in Figure 4.2 further reveals the behavior of CO₂ concentration in the whole process. The drop off in CO₂ concentration in Figure 4.2 comes from stopping the CO₂ from the inlet.

A linear interpolation was done to obtain an accurate amount of CO₂ release for a comparable data with Hadjisophocleous, Fu, and Lougheed [6]. It is also important to note that release rates for any fluids are extremely difficult to maintain a constant flow rates. Computer simulation models are able to maintain a more consistent and accurate flow rate.

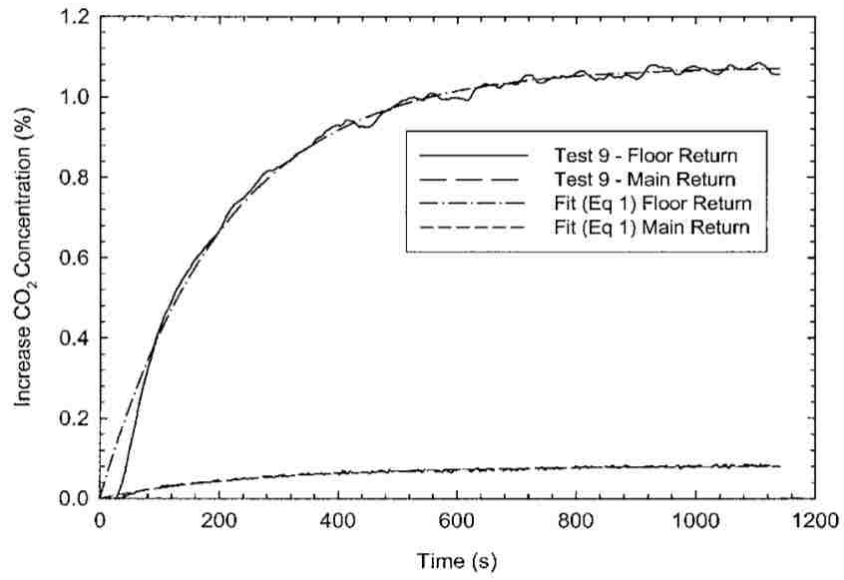


FIGURE 4.1. CO₂ concentration results from [6]

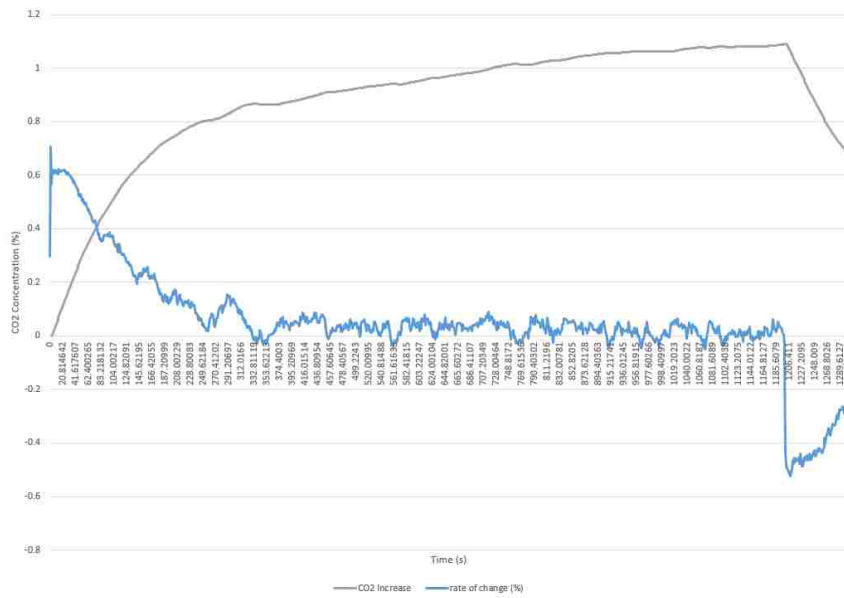


FIGURE 4.2. CO₂ concentration results produced by FDS

The blue line in Figure 4.2 shows the rate of change (in %) of CO₂ concentration, which is approximated by

$$f'(x_{j+1}) \approx \frac{f(x_{j+1}) - f(x_j)}{x_{j+1} - x_j}. \quad (4.1.1)$$

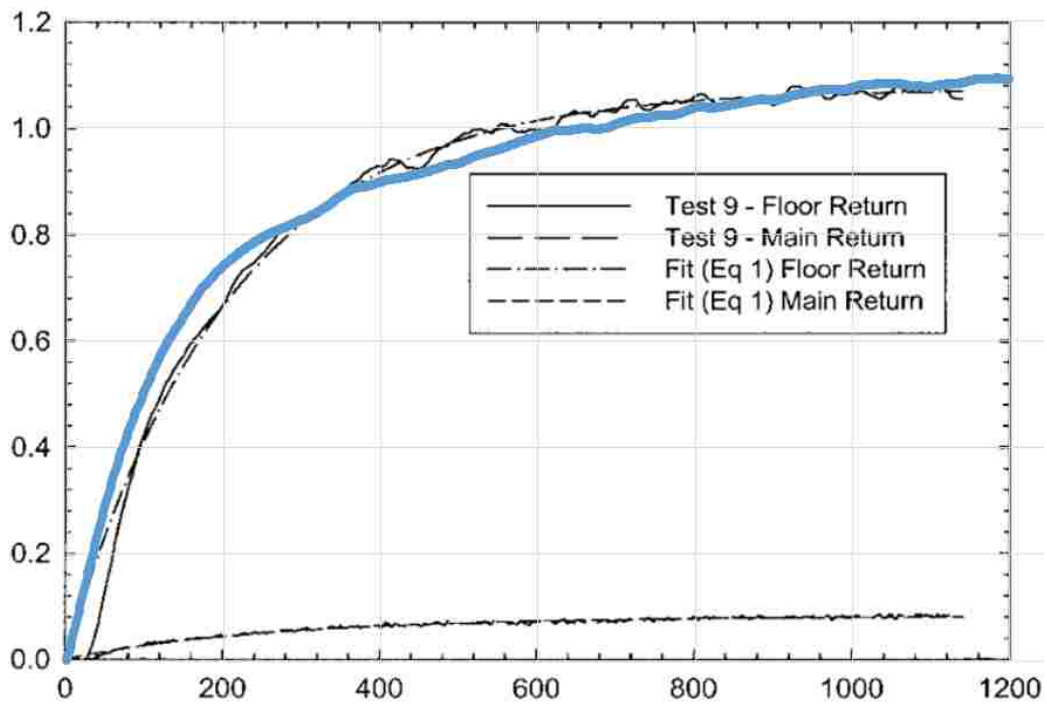


FIGURE 4.3. Simulated results in blue vs [6]

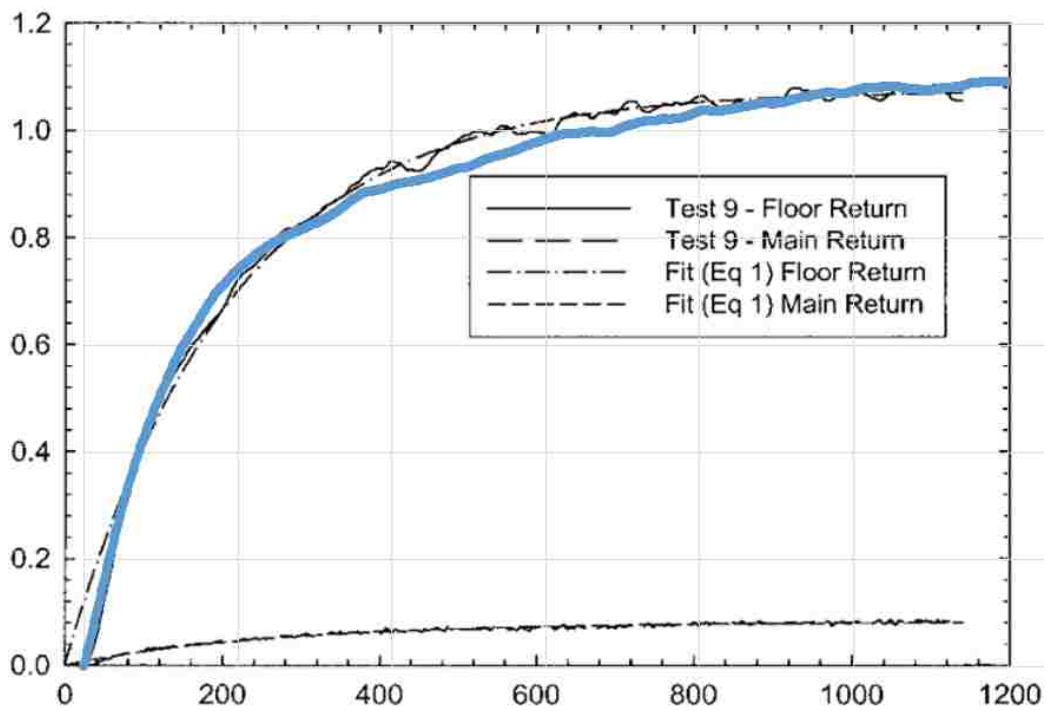


FIGURE 4.4. Simulated results in blue (shifted right) versus [6]

4.2. Temperatures at various heights.

The graphs for temperatures at various heights have fitted regression lines to give a R^2 value. Higher R^2 values indicated all of the variability of the response data is around its mean. This a lower R^2 value means that none of the variability of the response data is close to its mean. Which indicates how well a model fits the data when the differences between the observed values and predicted values are small and unbiased. Then correlation was found between the varying exhaust rates to see how strongly the temperatures at each height are related.

In Figures 4.5 - 4.19, temperature variations at different heights are seen along with different ventilation exhaust rates. From Figure 4.7 and Figure 4.8 we see a sudden jump in correlation value from 0.65 to 0.83. It can be said that as the fire continues to burn and time progresses the temperature and time relation is directly proportional. It's also seen that a similar jump in correlation in Figure 4.10 and Figure 4.11 from 0.73 to 0.84 along with Figure 4.15, Figure 4.16 and Figure 4.17. These jumps in correlation value show the dangers of fires regardless of fire size or fire power. Obviously, the more power the fire has, with 600 kW, extreme temperature jumps from 55°C to over 180°C are seen.

Notice that, once smoke and hot air reaches 5 meters in height the correlation drops slightly. From 4 meters in height to 5 meters in height due to the exhaust inlets on the ceiling. The temperatures for exhaust inlets extracting at 3 m³/s and 4 m³/s varies at 5 meters in height, which is the cause of the correlation value drop. It can be seen that when exhaust vents extract at a higher rate, the temperature can vary as much as 47°C.

By observation, the correlation is high for many of these figures at 3 and 4 meters high for heat release rates of 150kW, 300kW and 600kW. Which leads to a question, at what height is the correlation optimized and what is the reasoning behind it?

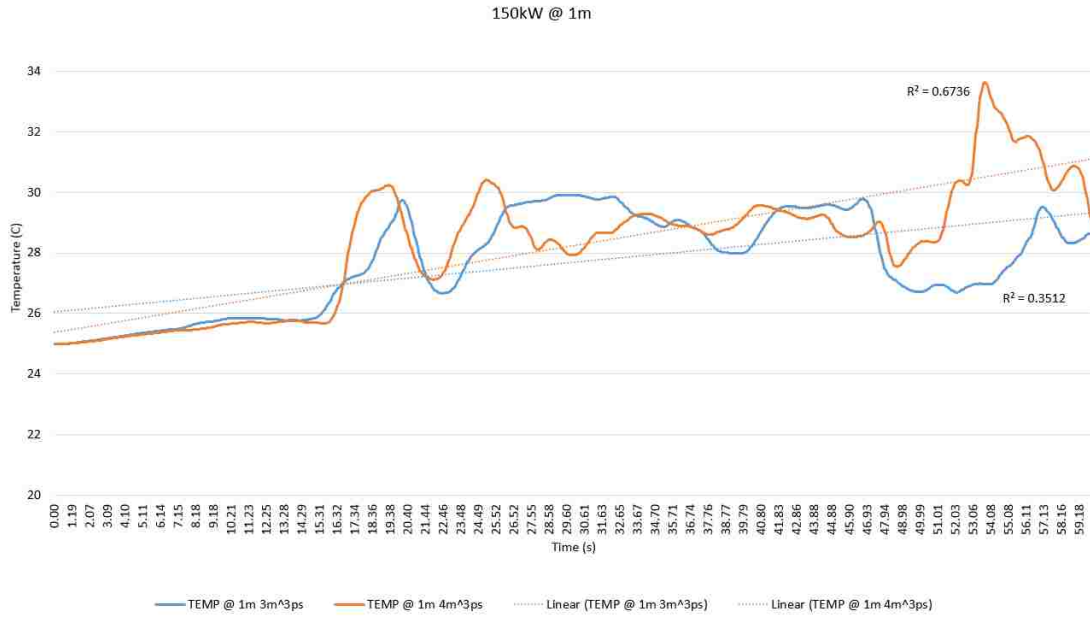


FIGURE 4.5. Exhaust vent: 3 - 4 m³/s, thermocouples at 1m, cor=0.656682

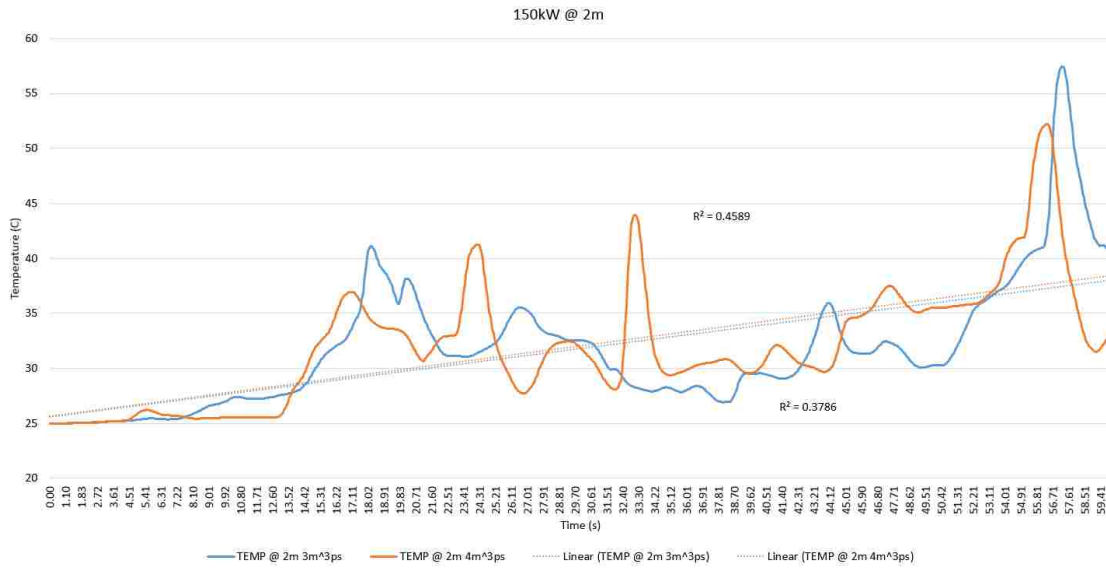


FIGURE 4.6. Exhaust vent: 3 - 4 m³/s, thermocouples at 2m, cor=0.655044

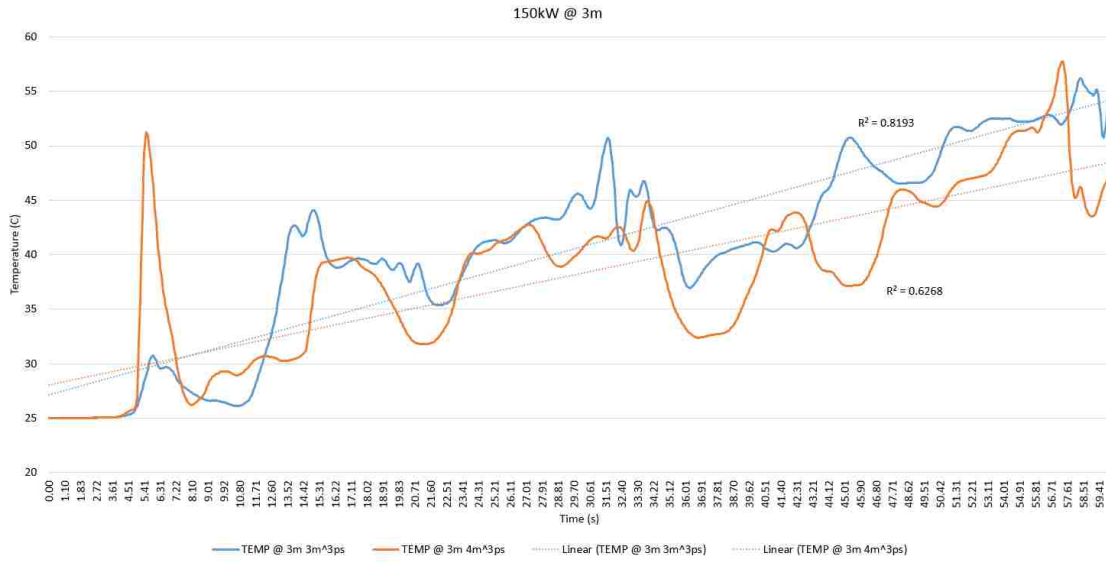


FIGURE 4.7. Exhaust vent: 3 - 4 m³/s, thermocouples at 3m, cor=0.655044

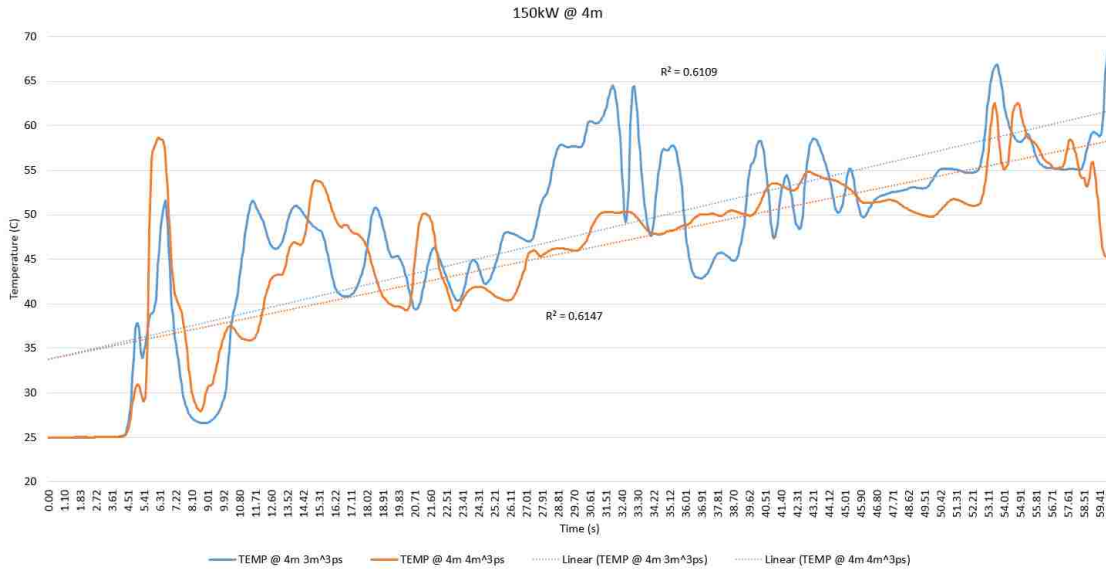


FIGURE 4.8. Exhaust vent: 3 - 4 m³/s, thermocouples at 4m, cor=0.831521

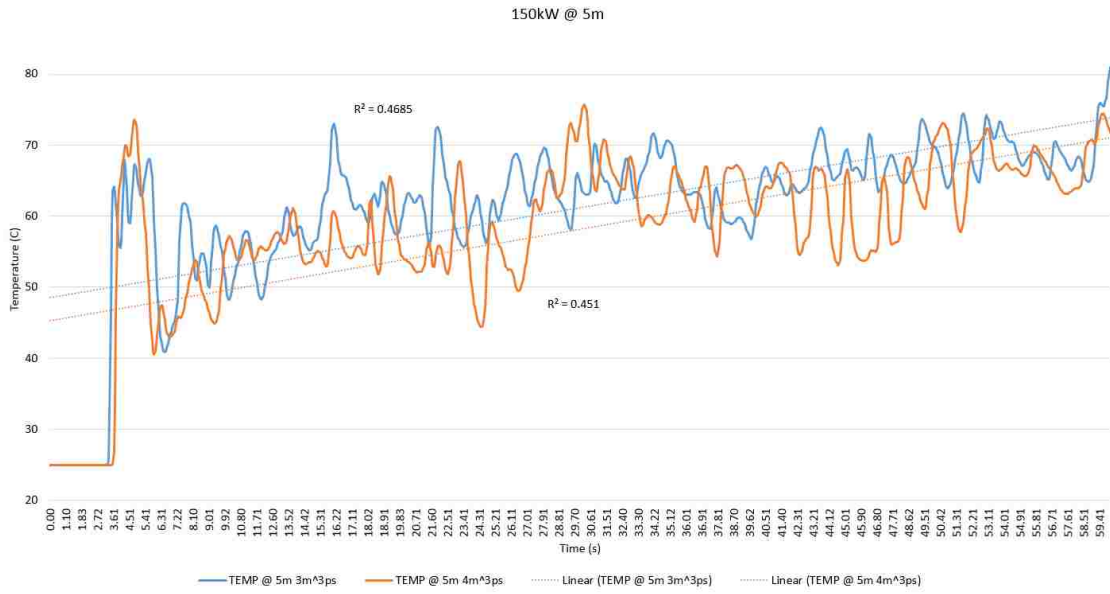


FIGURE 4.9. Exhaust vent: 3 - 4 m³/s, thermocouples at 5m, cor=0.799095



FIGURE 4.10. Exhaust vent: 3 - 4 m³/s, thermocouples at 1m, cor=0.736384

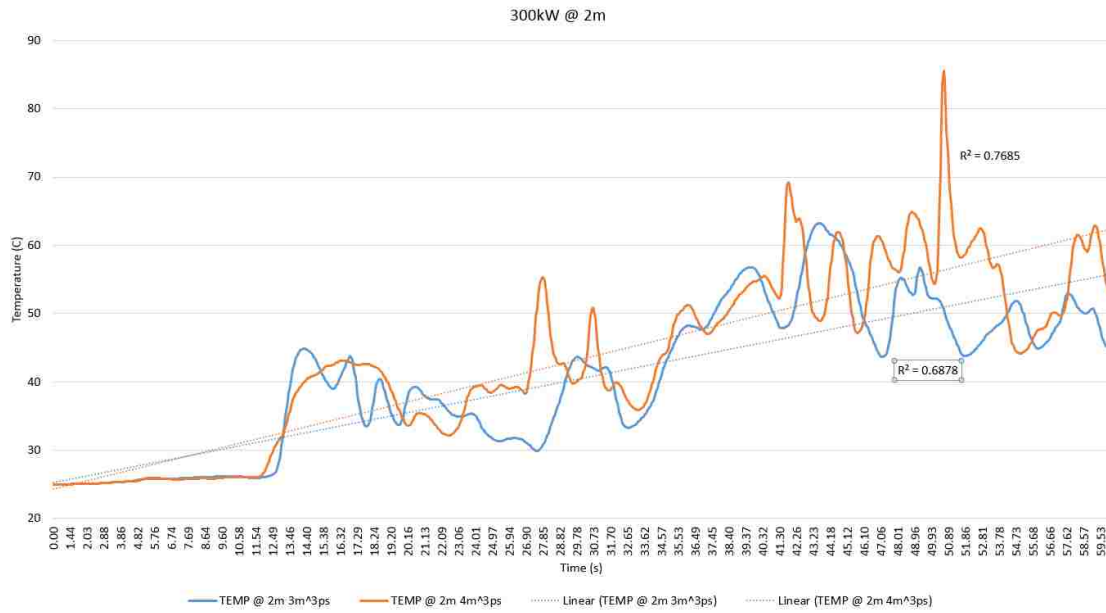


FIGURE 4.11. Exhaust vent: 3 - 4 m³/s, thermocouples at 2m, cor=0.846941

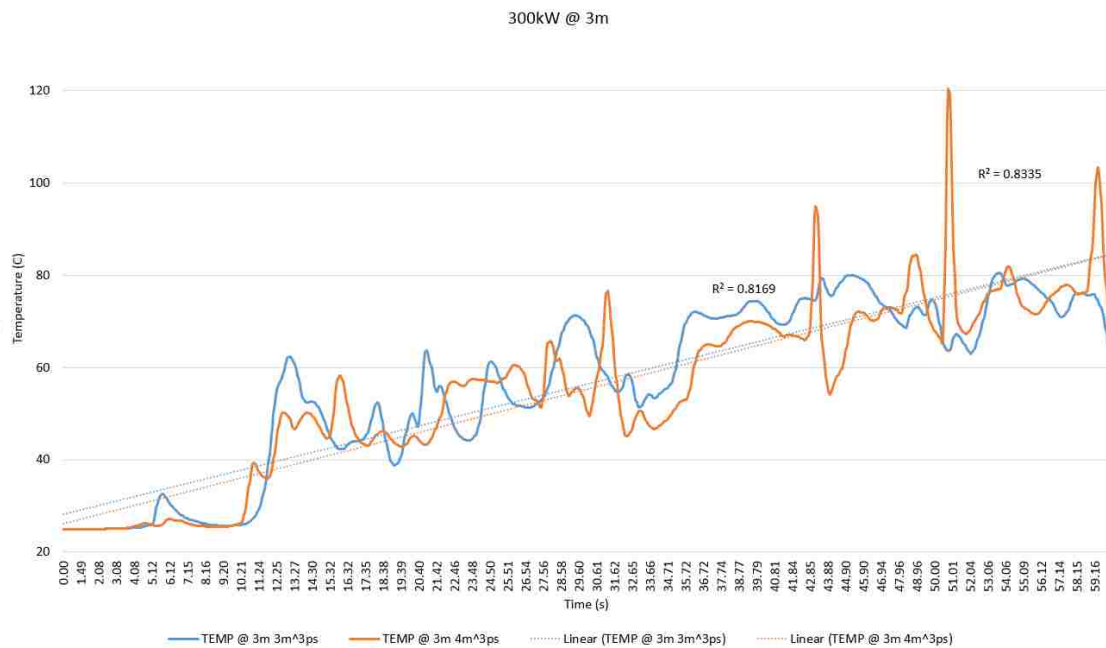


FIGURE 4.12. Exhaust vent: 3 - 4 m³/s, thermocouples at 3m, cor=0.884347

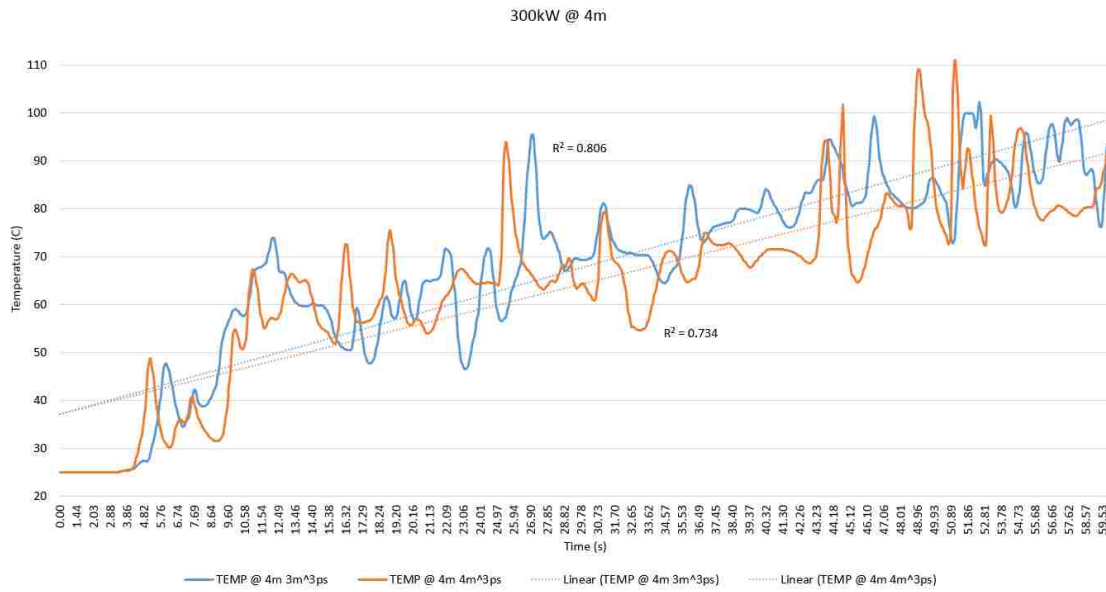


FIGURE 4.13. Exhaust vent: 3 - 4 m³/s, thermocouples at 4m, cor=0.858694

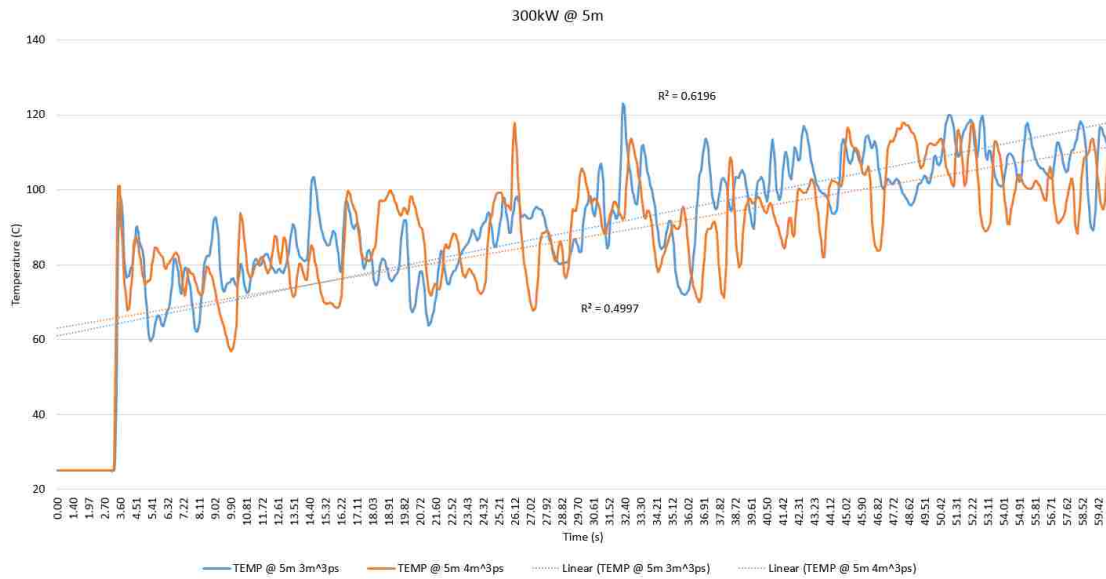


FIGURE 4.14. Exhaust vent: 3 - 4 m³/s, thermocouples at 5m, cor=0.82056

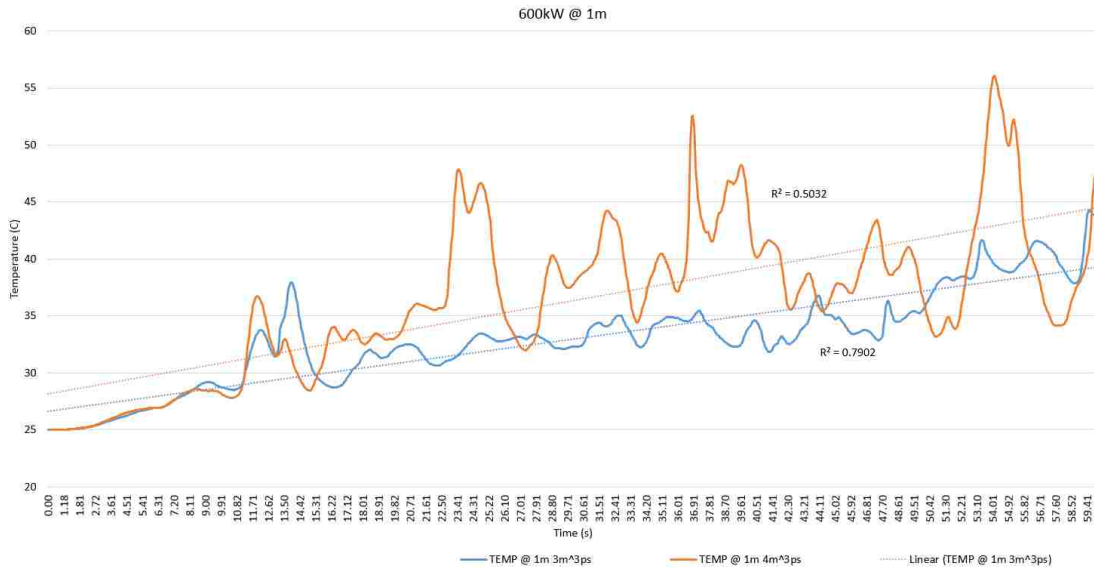


FIGURE 4.15. Exhaust vent: 3 - 4 m³/s, thermocouples at 1m, cor=0.668855

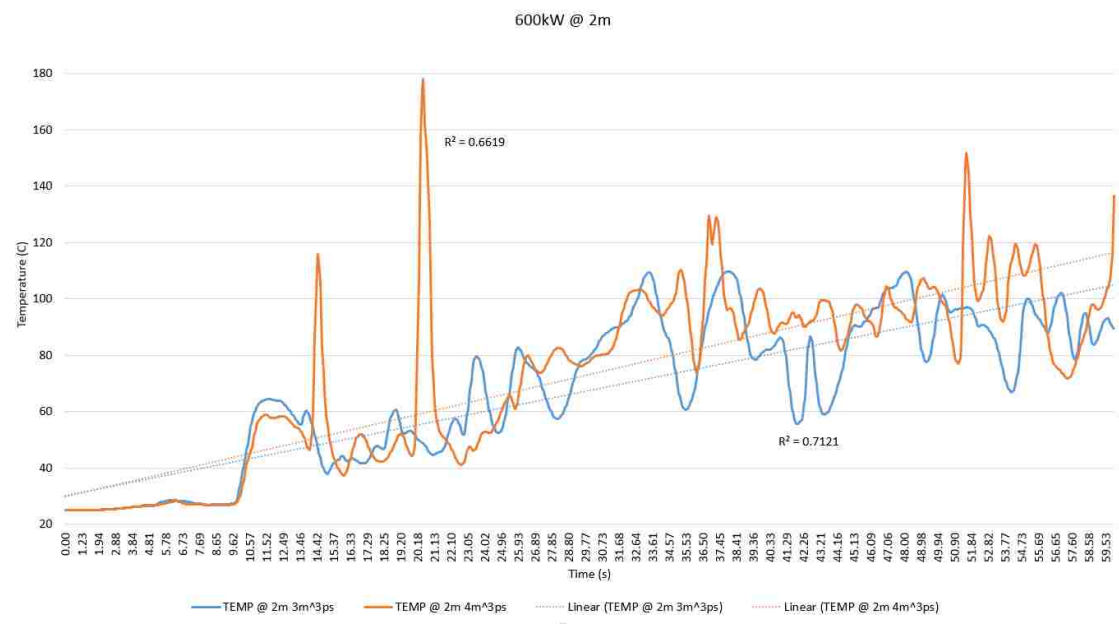


FIGURE 4.16. Exhaust vent: 3 - 4 m³/s, thermocouples at 2m, cor=0.792164

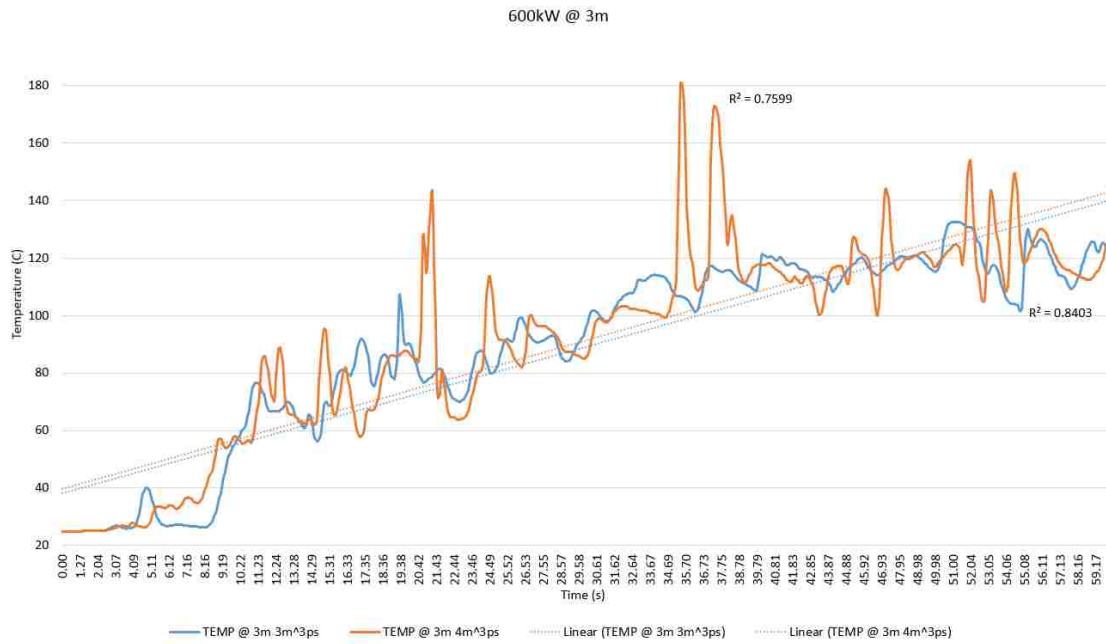


FIGURE 4.17. Exhaust vent: 3 - 4 m³/s, thermocouples at 3m, cor=0.914492

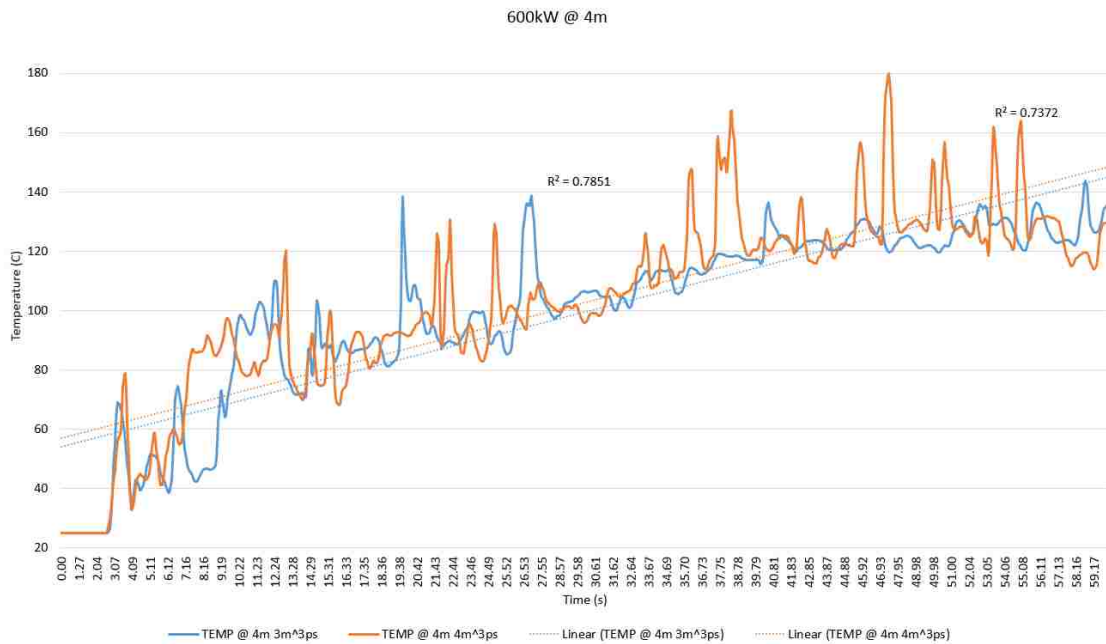


FIGURE 4.18. Exhaust vent: 3 - 4 m³/s, thermocouples at 4m, cor=0.876691

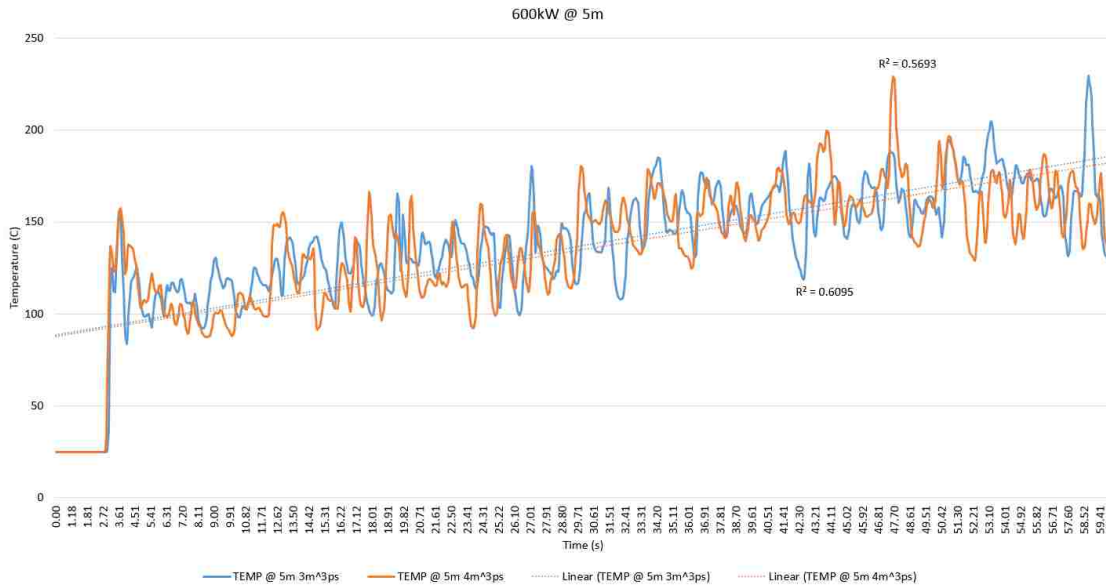


FIGURE 4.19. Exhaust vent: 3 - 4 m³/s, thermocouples at 5m, cor=0.840092

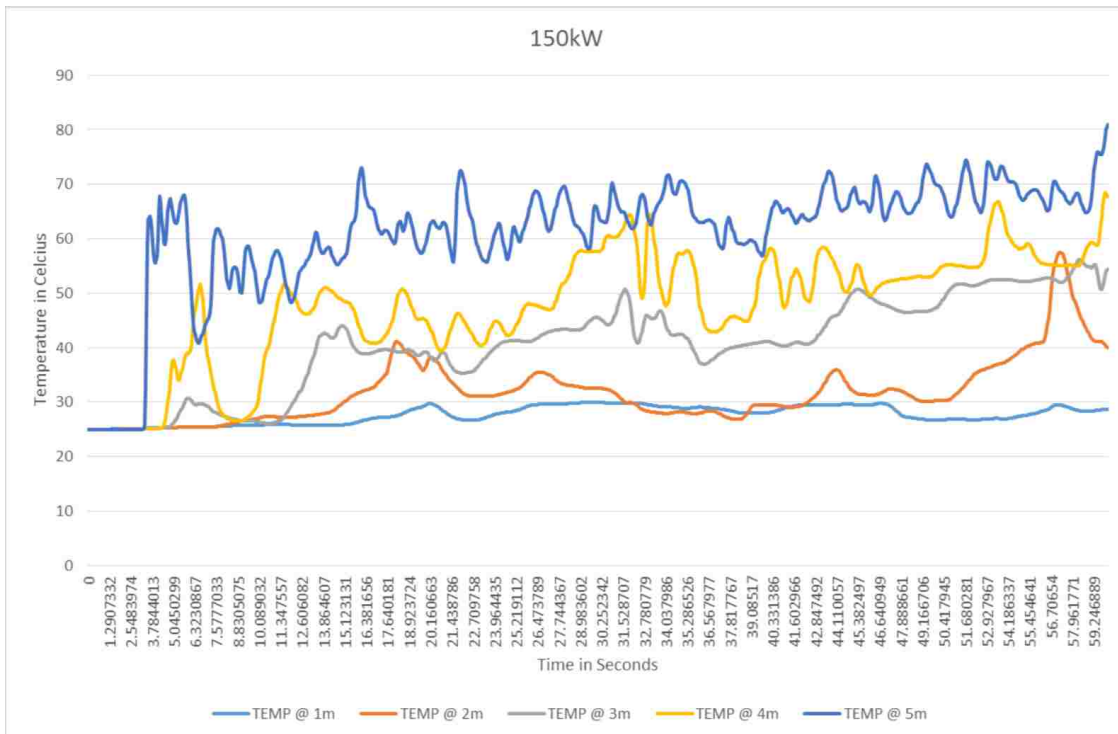


FIGURE 4.20. Exhaust vent: 3 m³/s. Thermocouples at 1 - 5m high

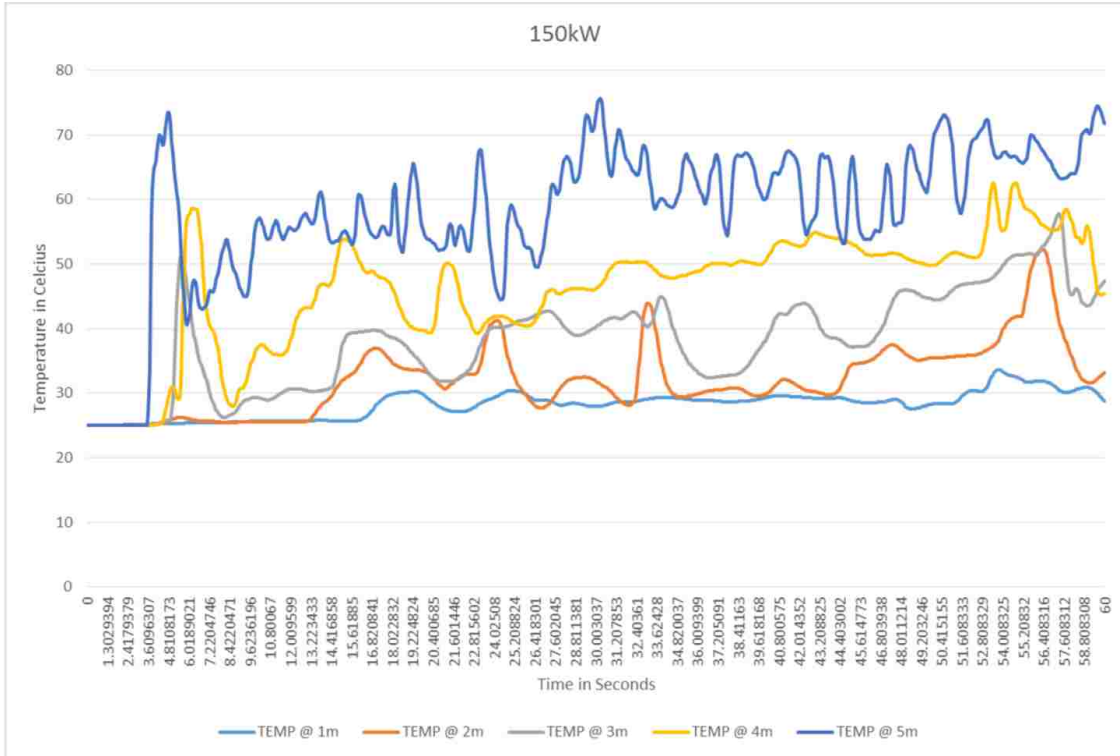


FIGURE 4.21. Exhaust vent: 4 m³/s. Thermocouples at 1 - 5m high

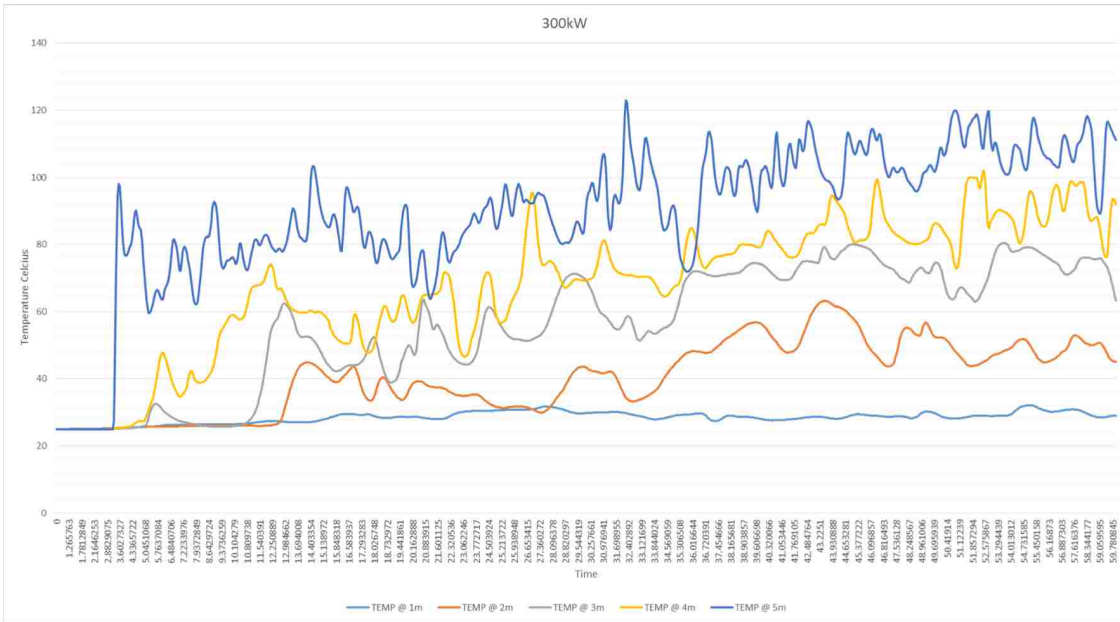


FIGURE 4.22. Exhaust vent: 3 m³/s. Thermocouples at 1 - 5m high

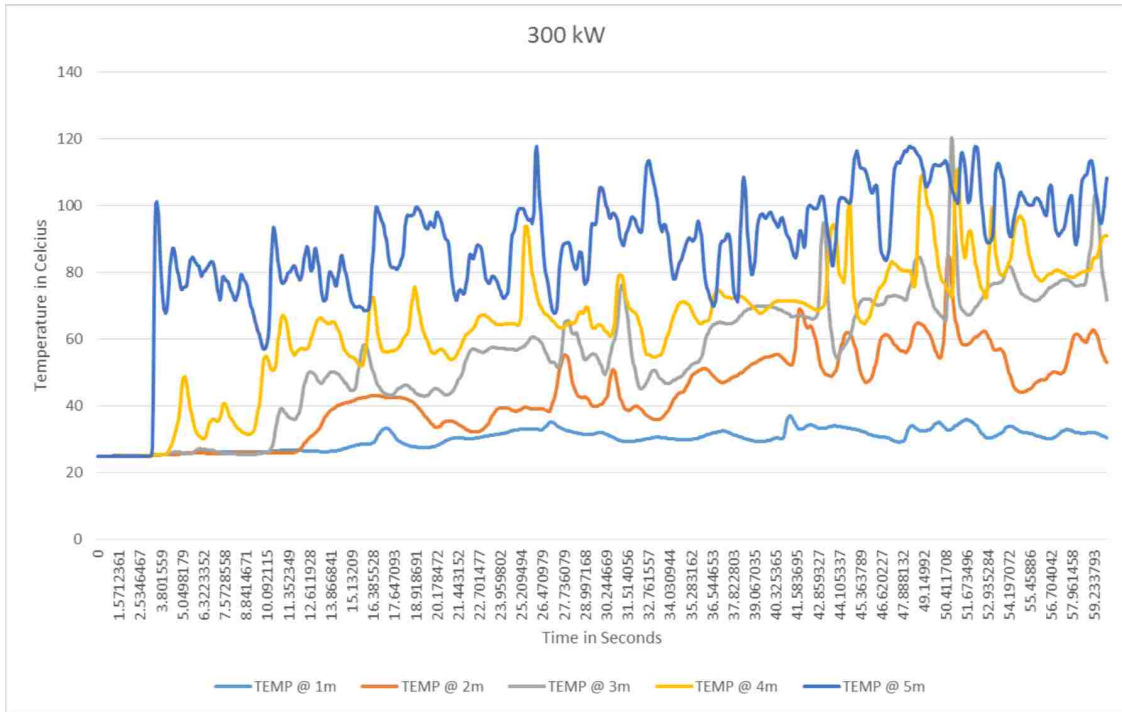


FIGURE 4.23. Exhaust vent: $4 \text{ m}^3/\text{s}$. Thermocouples at 1 - 5m high

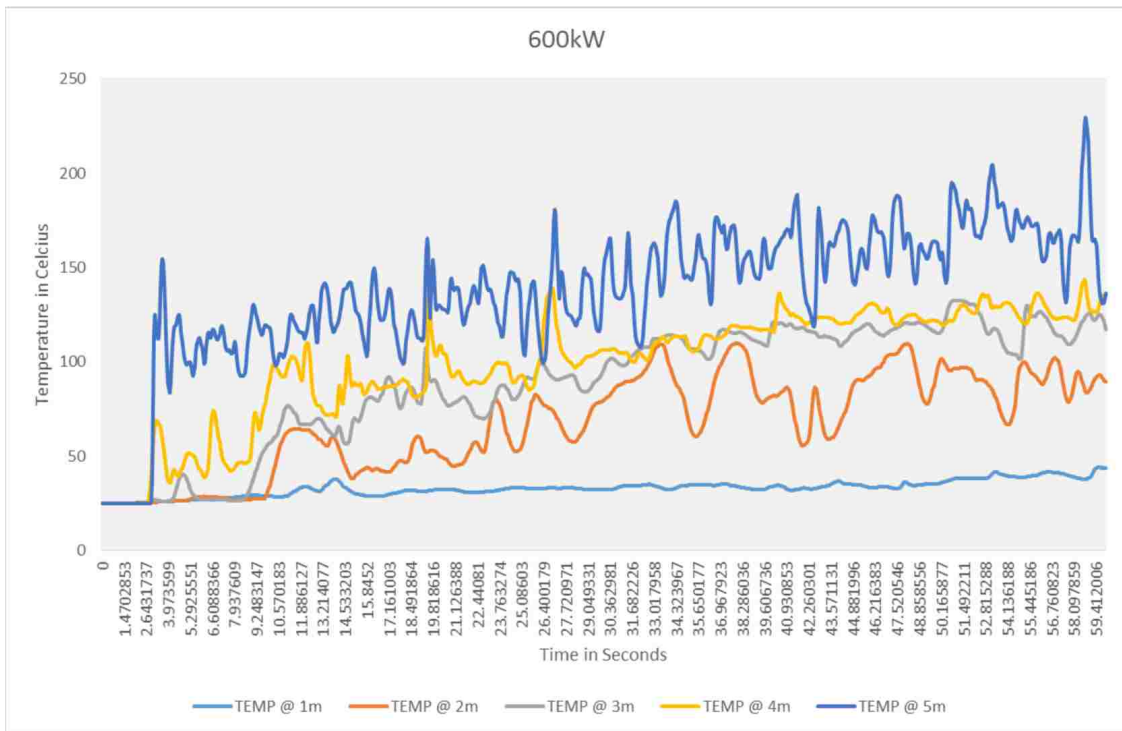


FIGURE 4.24. Exhaust vent: $3 \text{ m}^3/\text{s}$. Thermocouples at 1 - 5m high

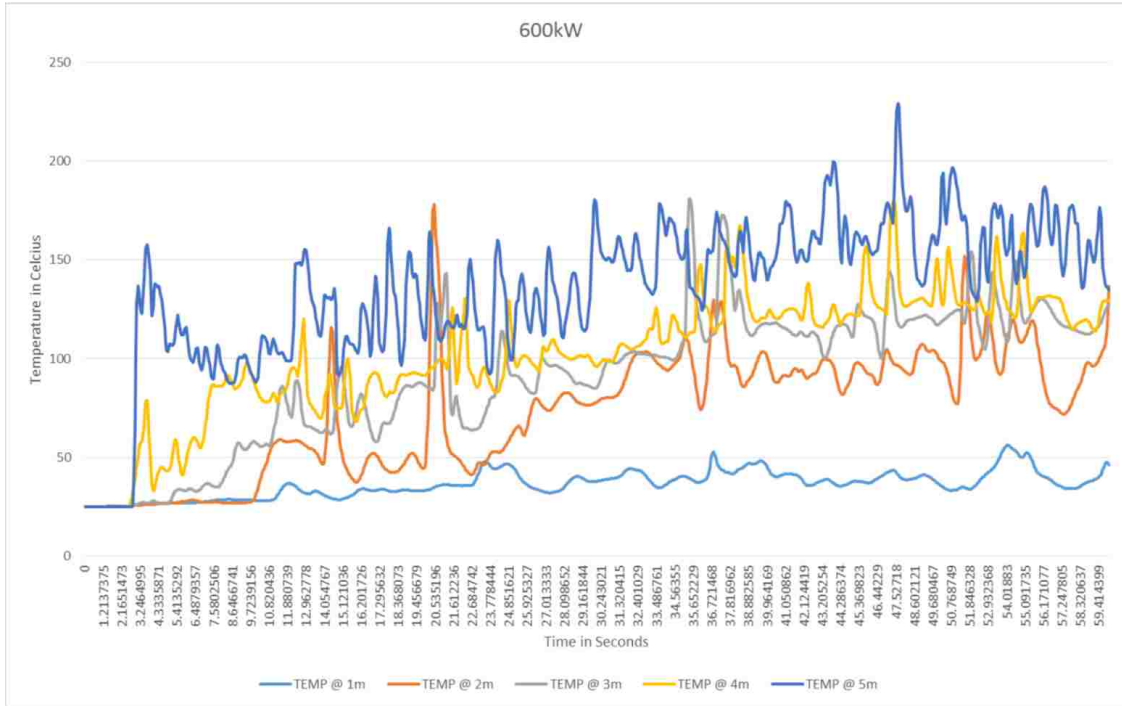


FIGURE 4.25. Exhaust vent: 4 m³/s. Thermocouples at 1 - 5m high

4.3. Heat release rates at various fire sizes.

In Figures 4.26 - 4.28 below, a lot of fluctuation occurs when FDS is trying to maintain the heat release rate at a steady state. It can also be observed that, the time it takes for FDS to reach the heat release rate is in under 2 seconds of simulation time. This must be taken in to consideration due to the fact that a fire starting from scratch takes significantly longer amount of time to reach any of the heat release rates tested in computer simulations.

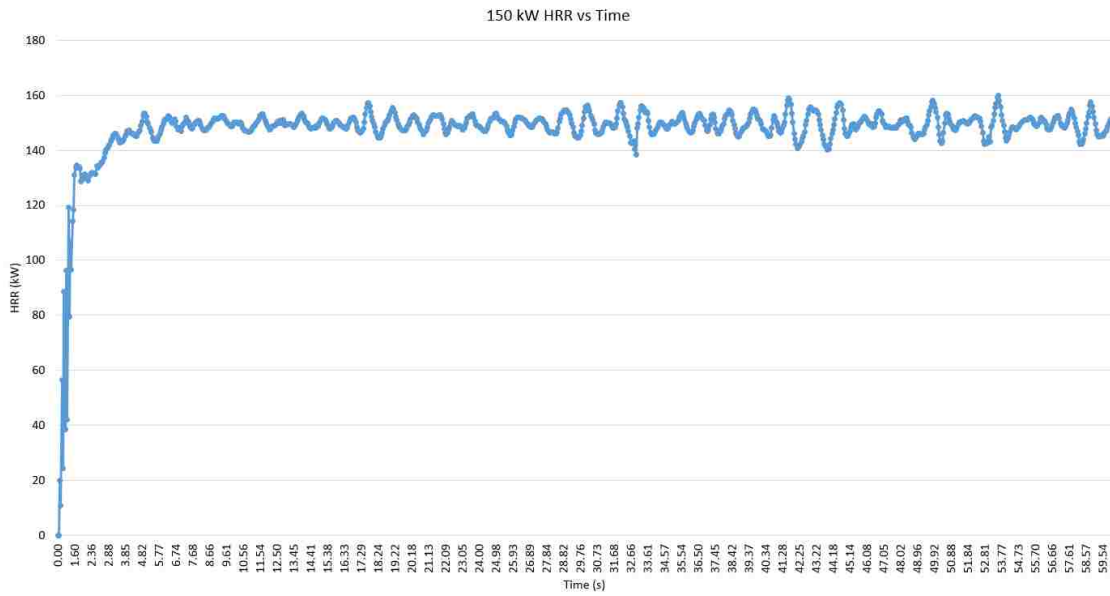


FIGURE 4.26. Heat release rate at 150kW

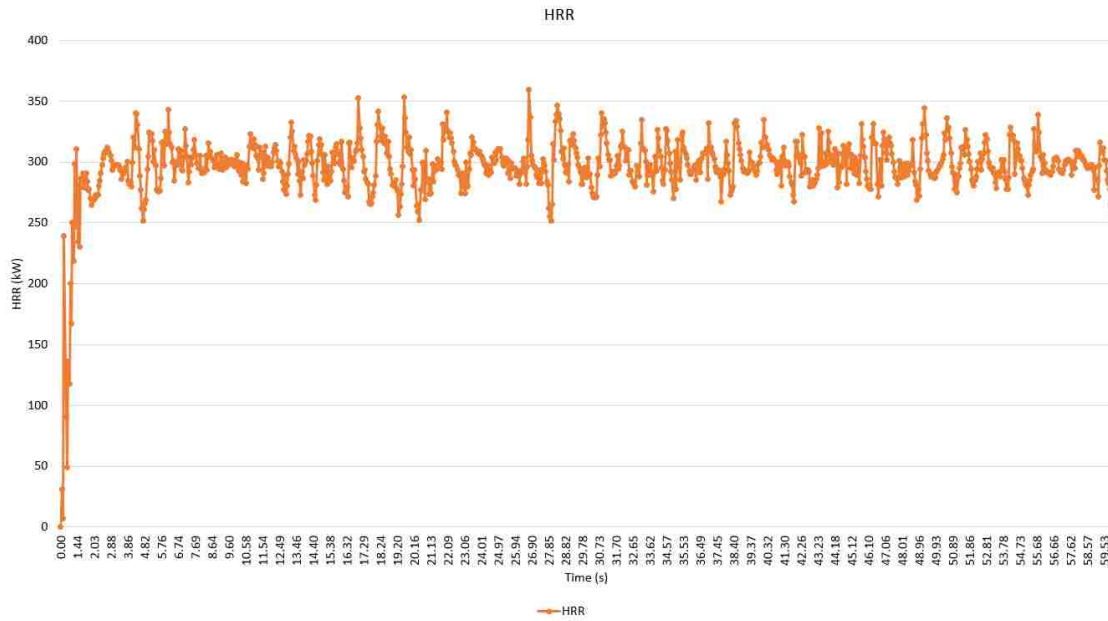


FIGURE 4.27. Heat release rate at 300kW

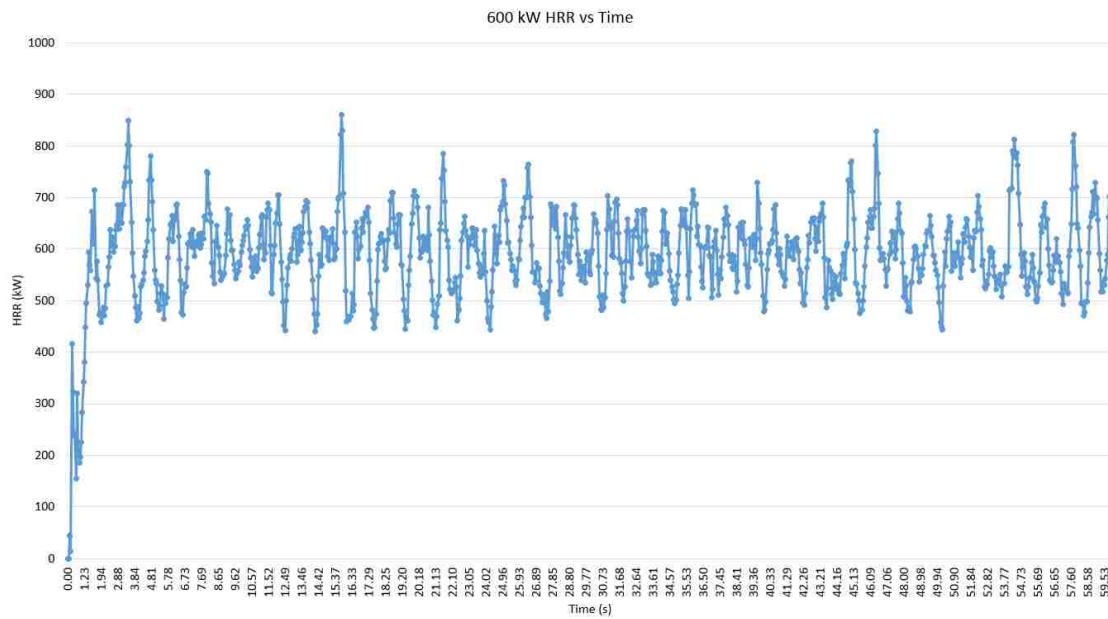


FIGURE 4.28. Heat release rate at 600kW

4.4. Temperature and Velocity Fields

Figures 4.29 through 4.36 are the temperature distributions. Figures 4.37 through 4.42 are the velocity distributions.

Currently, no literature can be found on specifically describing the behavior of smoke in an atrium. FDS has been able to give very detailed graphic of the velocity fields and temperature fields showing the behavior of smoke in an atrium and should have some empirical results to back up.

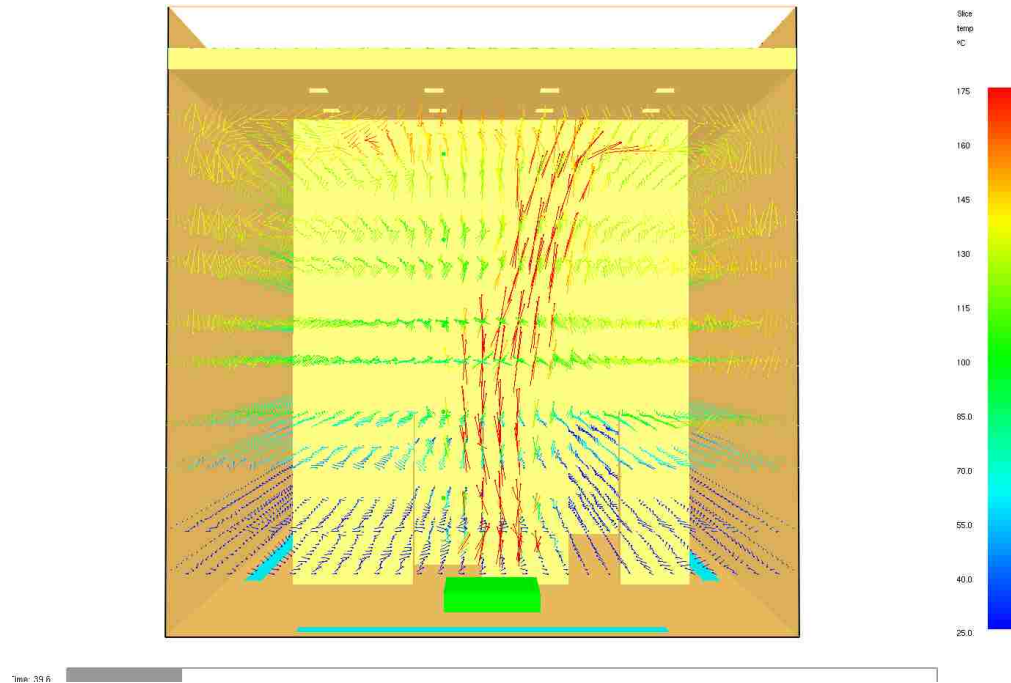


FIGURE 4.29. Temperature field in the z-plane

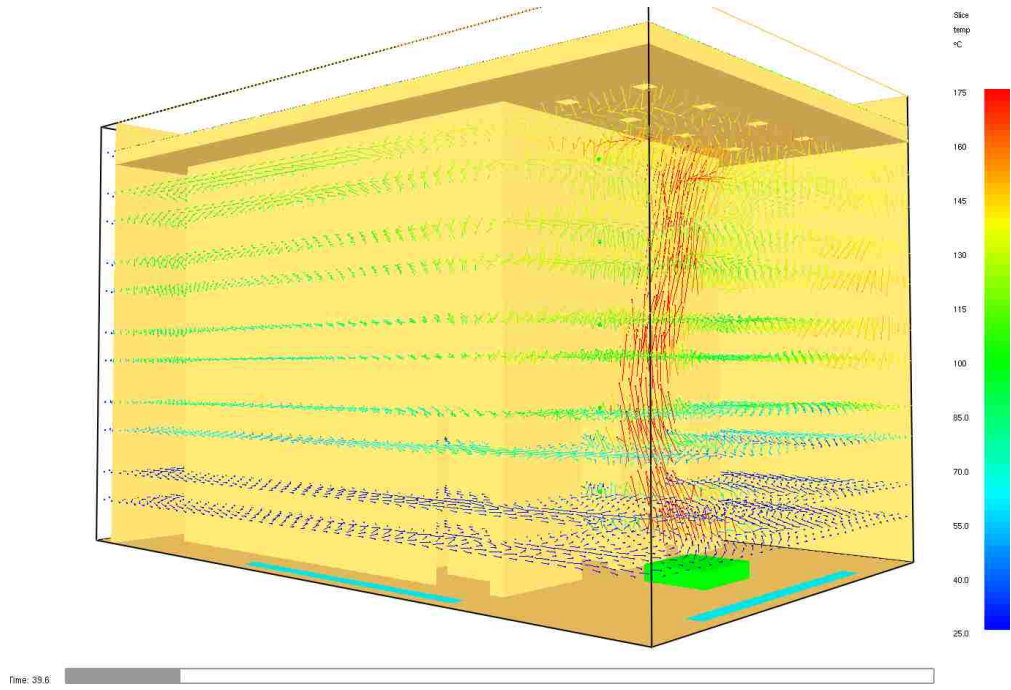


FIGURE 4.30. Temperature field in the z-plane

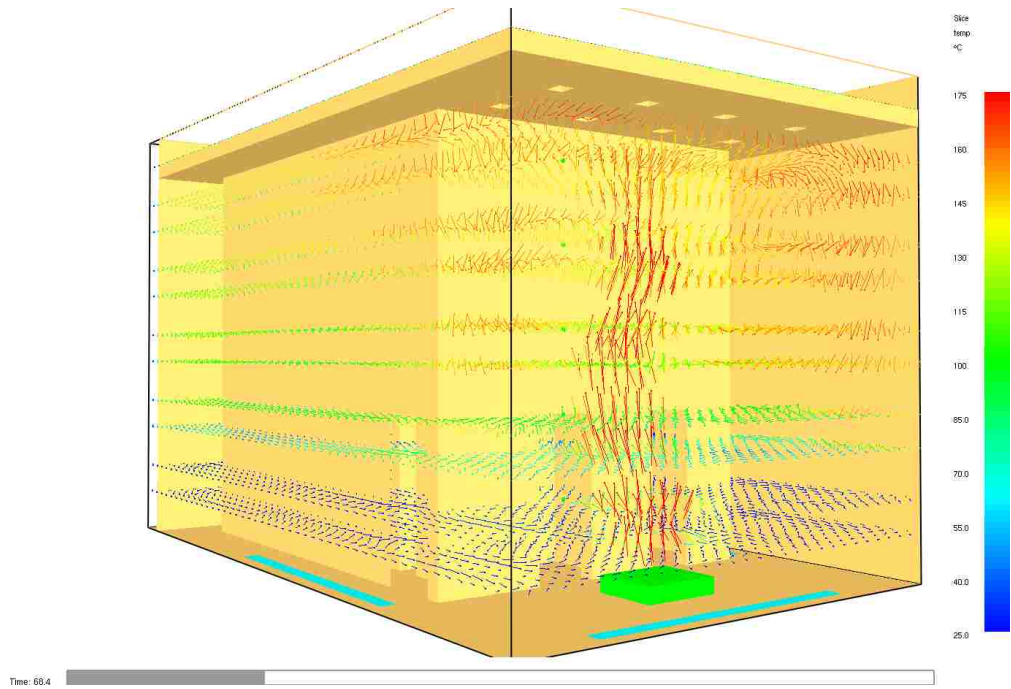


FIGURE 4.31. Temperature field in the z-plane

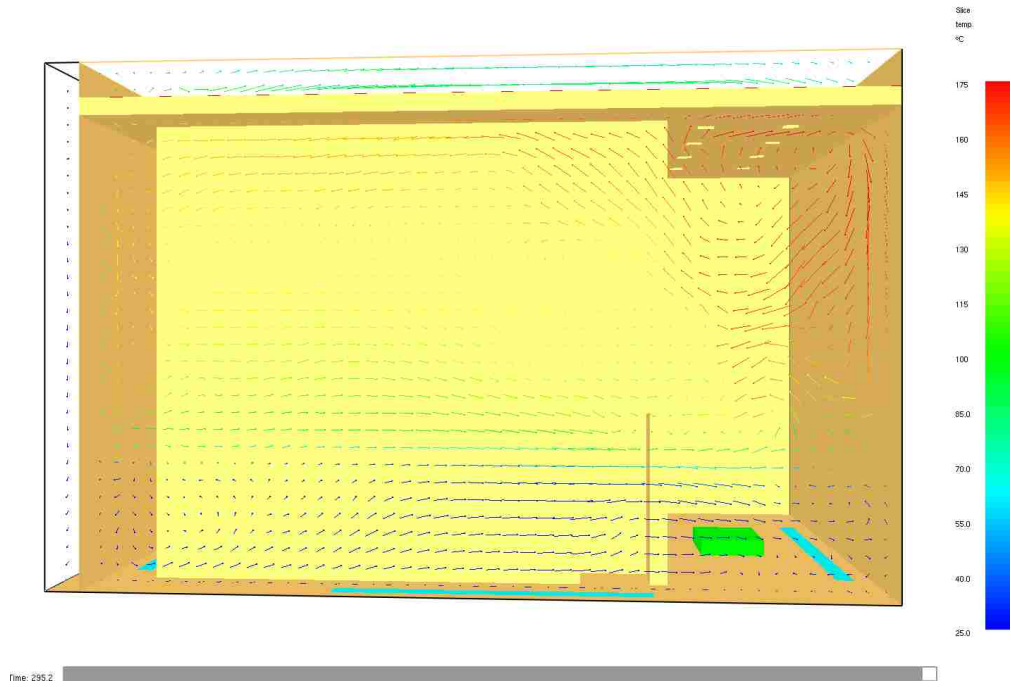


FIGURE 4.32. Temperature field in the y-plane

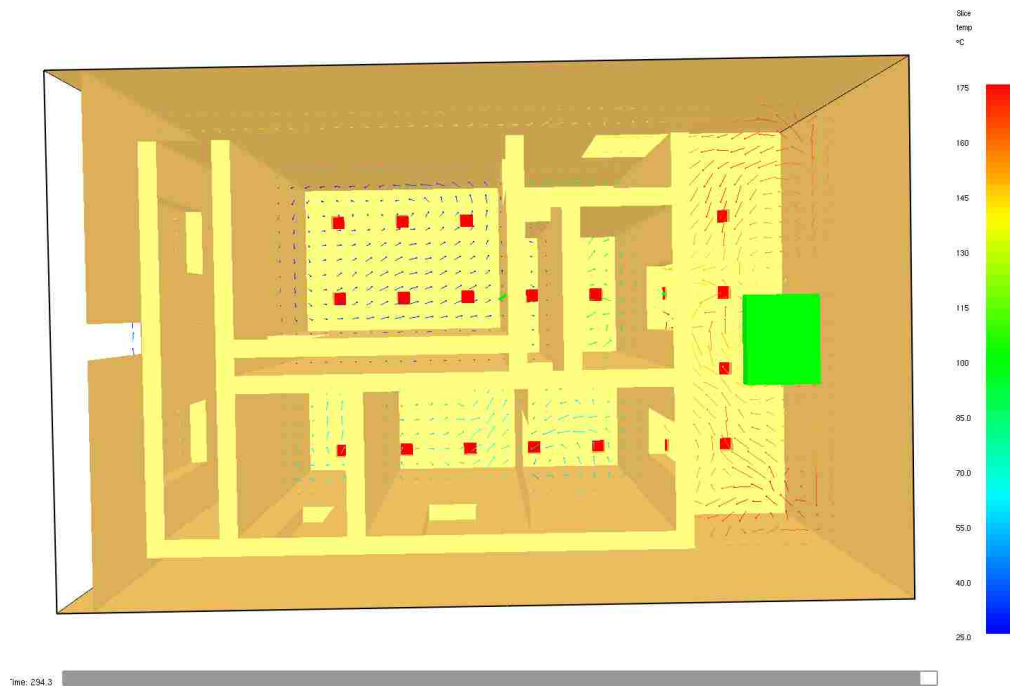


FIGURE 4.33. Temperature field in the z-plane

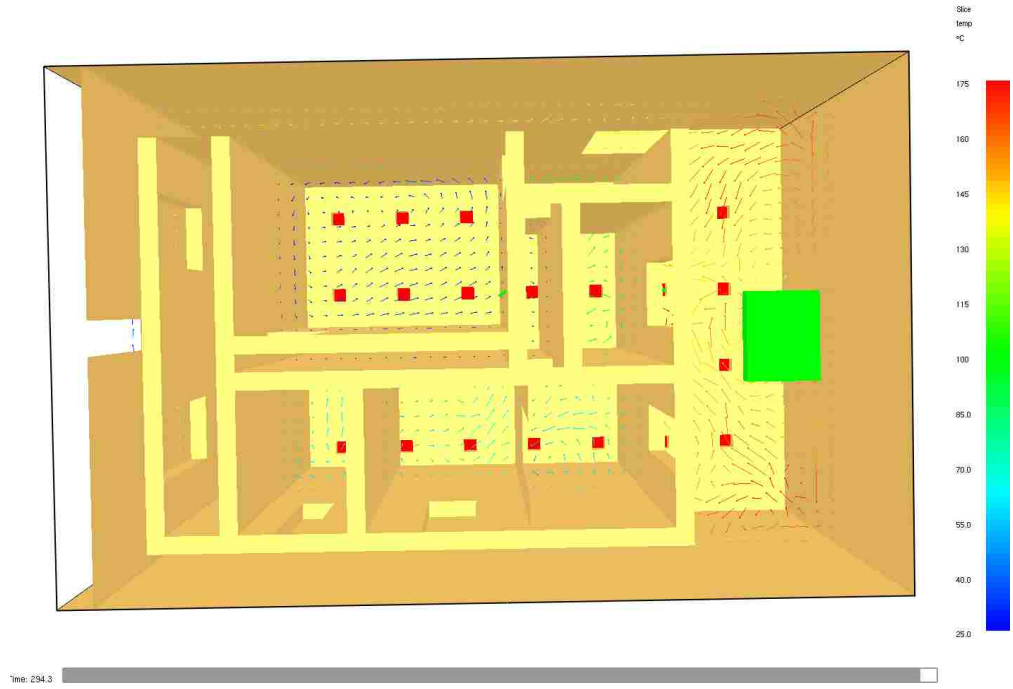


FIGURE 4.34. Temperature field in the z-plane

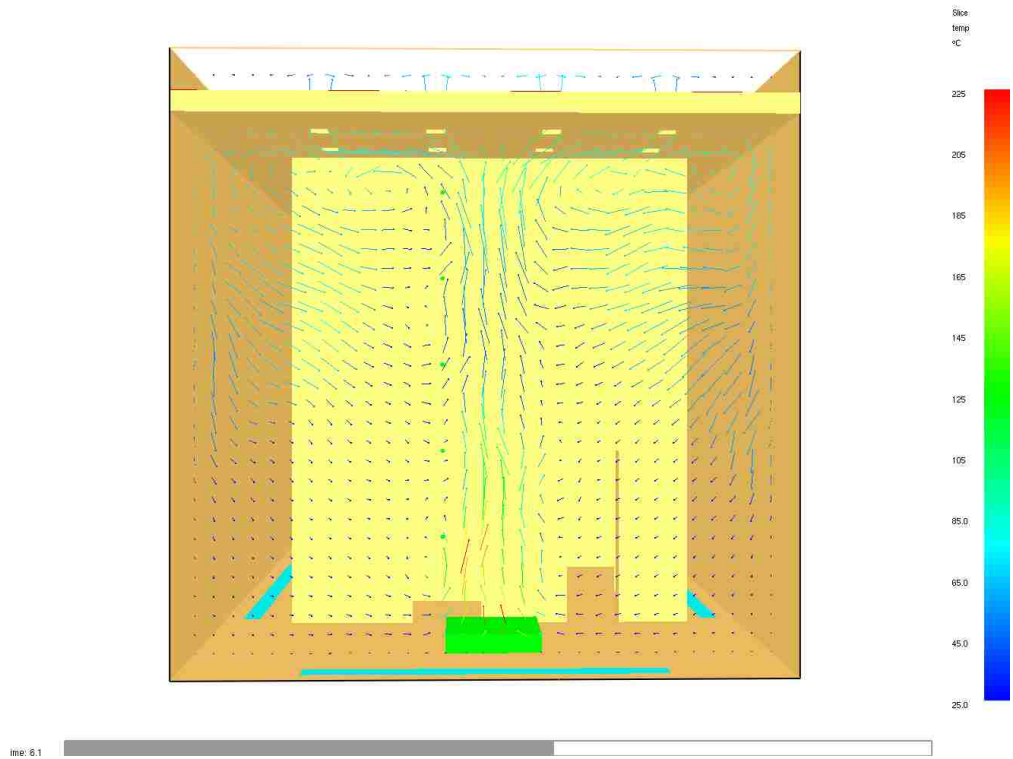


FIGURE 4.35. Temperature field in the x-plane

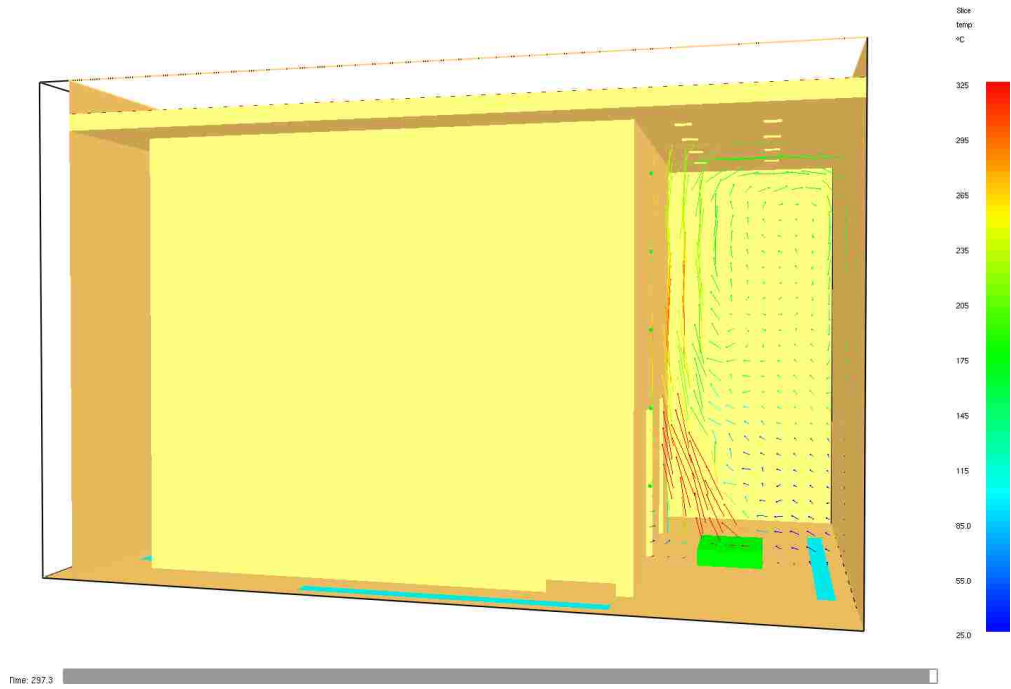


FIGURE 4.36. Temperature field in the y-plane

Since FDS does not consider flashovers, the exhaust system in the ceiling play a big factor in reducing the chances of flashovers. When the temperature in a room rises high enough from the billowing smoke and the radiating heat from the fire. This can cause as serious phenomena known as a flashover.

A flashover, is simultaneous ignition of combustible material in an enclosed area. According to wikipedia, flashovers occur around $500^{\circ}C$ to $590^{\circ}C$ [18] for most combustibles, such as furniture. The exhaust system reduces the heat within the atrium down to $280^{\circ}C$ mitigating a flashover.

As the smoke radiates to all the vertical walls after hitting the ceiling, this thermally induced movement according to J. H. McGuire [13], is know as the chimney effect. Stating that, the exterior pressure exceeds the interior pressure at lower levels and the opposite is true for higher levels. A neutral pressure plane occurs at the intermediate level, where the interior and exterior pressures are the same.

Currently, literatures on finding how to specifically described the behavior of smoke in an atrium has not been found. FDS has been able to give very graphic velocity fields of the behavior of smoke in an atrium and should have some empirical results to back it up.

Most buildings have mechanical ventilation systems that is mainly recirculating the air within. The smoke from fires within a building will disperse throughout. But that depends on if the fire region has outlets to other regions of the building. This can help with controlling the smoke in buildings.

Thus with the simulation model, more can be done on finding effective ways to funnel smoke into remote areas of the building is an area that could be looked in to more.

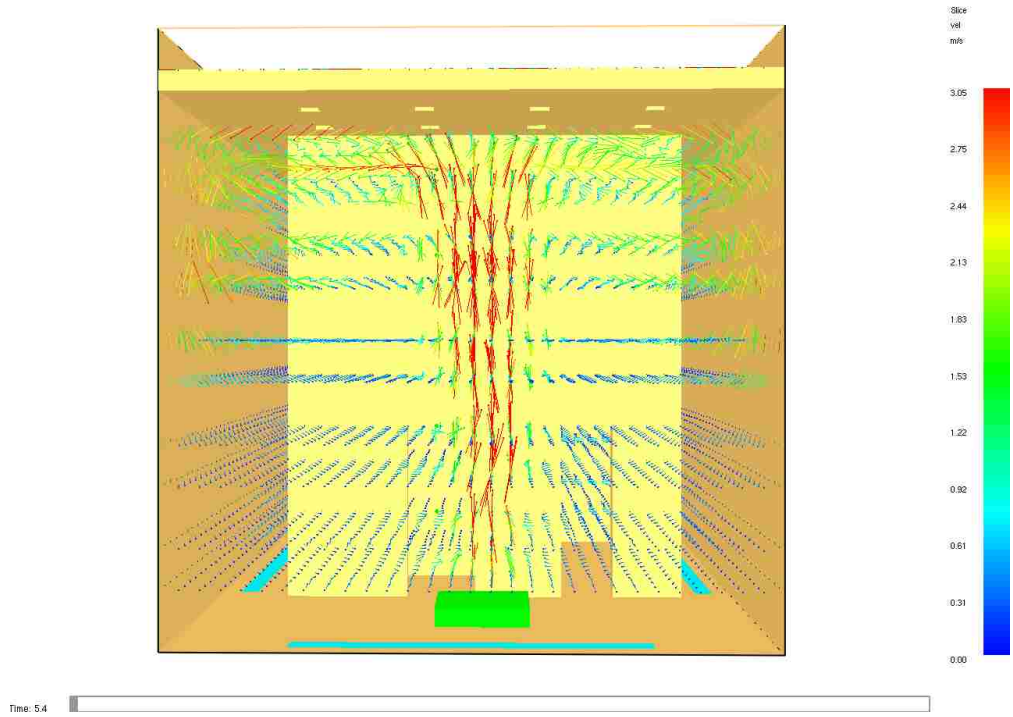


FIGURE 4.37. Velocity field in the z-plane

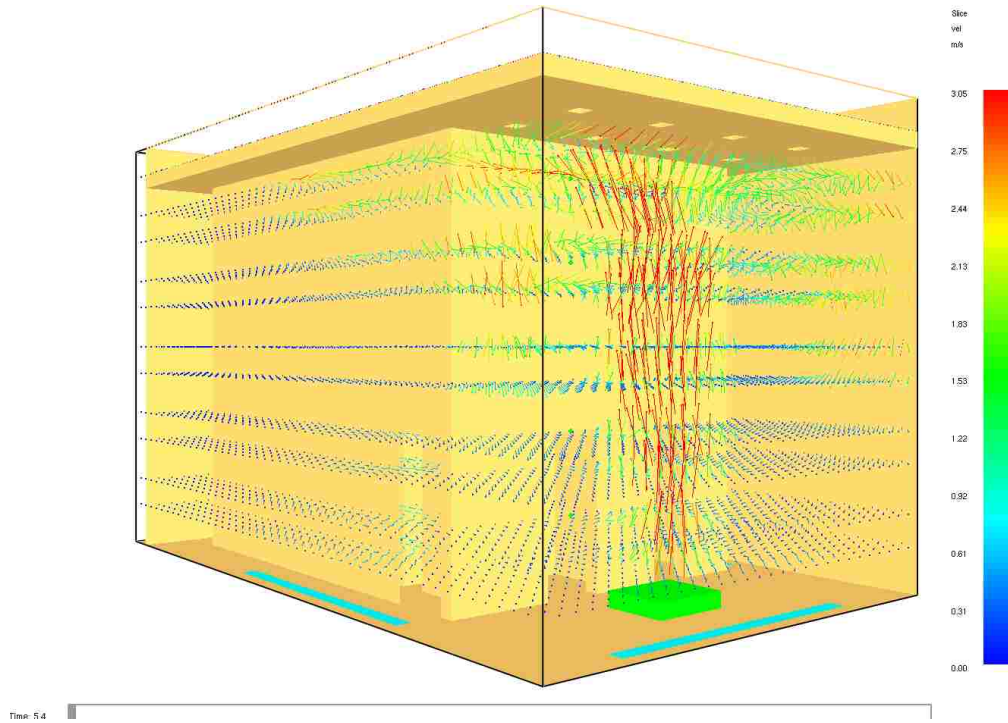


FIGURE 4.38. Velocity field in the z-plane

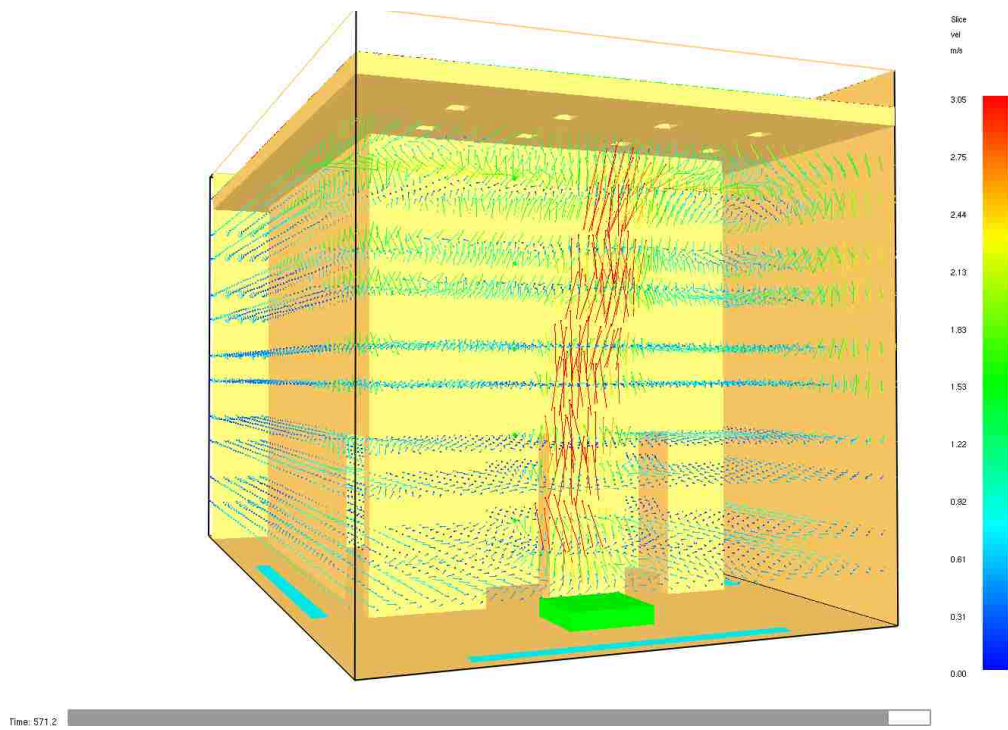


FIGURE 4.39. Velocity field in the z-plane

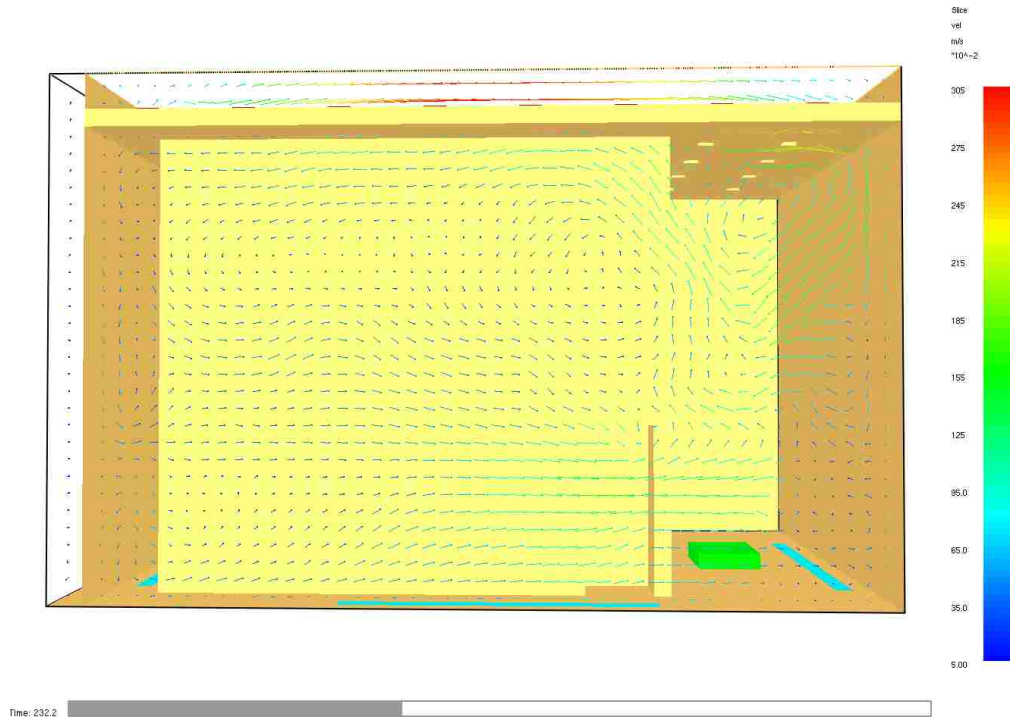


FIGURE 4.40. Velocity field in the y-plane

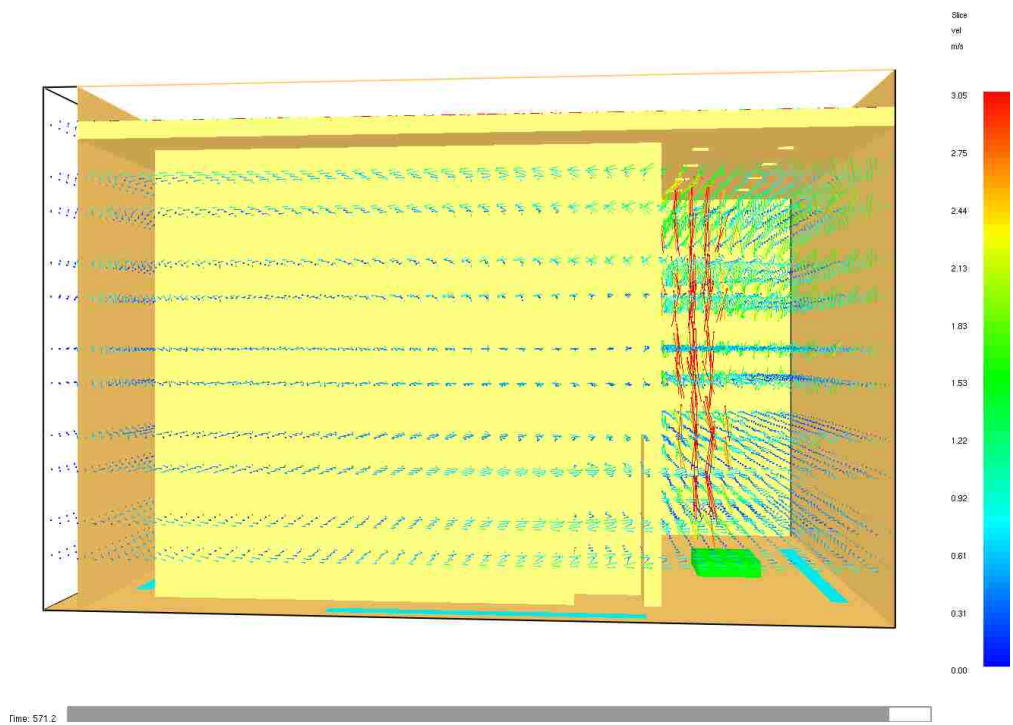


FIGURE 4.41. Velocity field in the y-plane

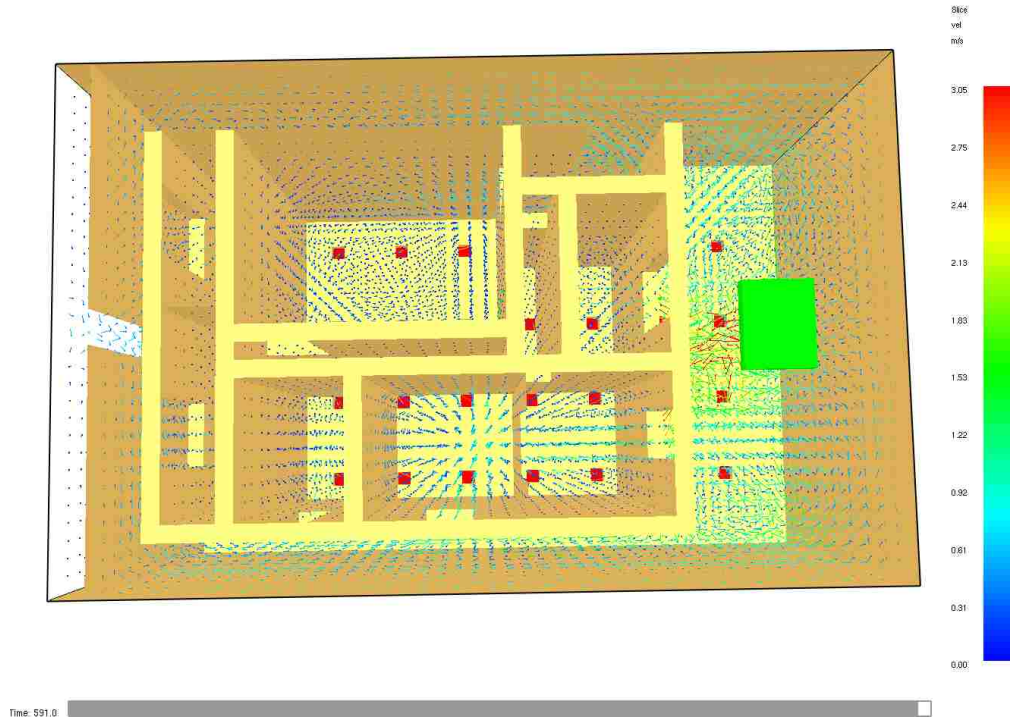


FIGURE 4.42. Velocity field in the z-plane

CHAPTER 5

FINAL REMARK

This paper presents computational fluid dynamic simulation data obtained from tests performed by FDS, to understand the effectiveness of smoke exhaust systems in atriums. The data shows results that compare well with experimental data, from Hadjisophocleous's two zone model [6] with the CO₂ concentration.

The varying exhaust rates do not tell much about the lower layer and upper layers of smoke. But, there is a interesting phenomenon in each of the varying heat release rate at 3 to 4 meters high, the correlation increase higher than at other heights.

The computer used, had 4 CPUs, 1.8GHz processor with 32GB of ram. FDS with 342,000 nodes and a heat release rate of 600 kW, took over 104 hours to finish a simulation time of 600 seconds and 153 hours of CPU time.

Finding more cost effective way to solve LES models would greatly advance the understanding of smoke movement to help aid in rescues and fire fighter. Also adding randomization factor for smoke would make the simulation more realistic. Fires are very hard to predict.

Most buildings and homes ventilation systems mainly recycle the air within instead of drawing most of the air from outside. This will cause further issues during a fire when the ventilation system kicks on as heavy smoke is release into the building. This would further blast smoke to places of least desirability during a fire. Designing a system that fail safes to only exhaust the gases within the building or to fail safe off completely would allow better control of smoke flow.

Since, no literatures has been found on describing smoke behavior in an atrium in terms of velocity and temperature fields, an empirical or experimental study is necessary to backup the results from FDS. Designing such an experiment won't be easy.

APPENDIX A

DFS CODE FOR THIS THESIS

```
1 &HEAD CHID=?ATRIUM? , TITLE=?Test? /
2
3 &MESH IJK=47.5,30,30, XB=0,9,0,6,0,5.5 /
4 &RADI RADIATION=.TRUE. /
5 &TIME T_END=1300 /
6
7 &MISC TMPA=25. /
8
9 &SURF ID= 'BURNER' , HRRPUA= '600' , COLOR= 'YELLOW' /
10 &REAC SOOT_YIELD=0.03 , FUEL="PROPANE" /
11 &MATL ID                = 'INSULATION'
12     DENSITY              = 130
13     CONDUCTIVITY         = 0.08
14     SPECIFIC_HEAT        = 0.9
15     EMISSIVITY           = 0.9 /
16
17 &SURF ID                = 'WALL'
18     MATL_ID              = 'INSULATION'
19     THICKNESS            = 0.025 /
20
21
22 &SPEC ID= 'CARBON_DIOXIDE' /
23 &SURF ID="LEAK" , SPEC_ID= 'CARBON_DIOXIDE' , MASS_FLUX=0.025 , RAMP_MF(1)=
24     leak_ramp' /
25 &RMP ID= 'leak_ramp' , T= 0. , F=0.0 /
26 &RMP ID= 'leak_ramp' , T= 1. , F=1.0 /
27 &RMP ID= 'leak_ramp' , T=1200. , F=1.0 /
```

```

28 &RMP ID='leak_ramp', T=1201., F=0.0 /
29 &VENT XB=4.55,4.55,2.55,3.15,0,0.5, SURF_ID='LEAK', COLOR='RED' /
30 &DMP MASS_FILE=.TRUE. /
31 &SLCF PBX=0.00, QUANTITY='MASS_FRACTION', SPEC_ID='CARBON_DIOXIDE' /
32
33
34
35
36 &DEVC XYZ=4.55,2.55,1.0, 'QUANTITY='TEMPERATURE', ID='TEMP @ 1m sw' /
37 &DEVC_XYZ=4.55,2.55,2.0, 'QUANTITY='TEMPERATURE', ID='TEMP_@_2m_sw' /
38 &DEVC XYZ=4.55,2.55,3.0, 'QUANTITY='TEMPERATURE', ID='TEMP @ 3m sw' /
39 &DEVC_XYZ=4.55,2.55,4.0, 'QUANTITY='TEMPERATURE', ID='TEMP_@_4m_sw' /
40 &DEVC XYZ=4.55,2.55,5.0, 'QUANTITY='TEMPERATURE', ID='TEMP @ 5m sw' /
41
42
43
44 &DEVC_XYZ=6.59,2.55,1.0, 'QUANTITY='TEMPERATURE', ID='TEMP_@_1m' /
45 &DEVC XYZ=6.59,2.55,2.0, 'QUANTITY='TEMPERATURE', ID='TEMP @ 2m' /
46 &DEVC_XYZ=6.59,2.55,3.0, 'QUANTITY='TEMPERATURE', ID='TEMP_@_3m' /
47 &DEVC XYZ=6.59,2.55,4.0, 'QUANTITY='TEMPERATURE', ID='TEMP @ 4m' /
48 &DEVC_XYZ=6.59,2.55,5.0, 'QUANTITY='TEMPERATURE', ID='TEMP_@_5m' /
49
50
51 &OBST XB=7.09,8.09,2.5,3.5,0,0.2,COLOR='GREEN',SURF_IDS='BURNER','INERT','
52     INERT' /
53
54 &OBST XB=-0.11,0,0,6,0,5.5,SURF_ID='WALL',TRANSPARENCY=1/ FRONT
55     OF BUILDING
56 &HOLE XB=-0.11,0,2.73,3.28,0,2 / FRONT DOOR
57

```

58 &OBST XB=0.61,6.49,0.73,0.85,0,5.5,SURF_ID='WALL',TRANSPARENCY=0 /
59 FRONT SIDE

60 &OBST XB=0.61,6.49,5.25,5.37,0,5.5,SURF_ID='WALL',TRANSPARENCY=0 /
61 BACK SIDE

62 &OBST XB=0.61,0.72,0.73,5.25,0,5.5,SURF_ID='WALL',TRANSPARENCY=0 /
63 LEFT SIDE

64 &OBST XB=6.47,6.58,0.73,5.25,0,5.5,SURF_ID='WALL',TRANSPARENCY=0 /
65 RIGHT SIDE

66 &OBST XB=0,9,0,6,5.475,5.575,SURF_ID='WALL',TRANSPARENCY=0 /
67 CEILING

68

69 &OBST XB=0.61,1.4,2.73,2.85,0,5.5,SURF_ID='WALL',TRANSPARENCY=0 /
70 &OBST XB=1.4,1.51,0.73,5.27,0,5.5,SURF_ID='WALL',TRANSPARENCY=0 /
71 &OBST XB=1.4,6.49,3.46,3.58,0,5.5,SURF_ID='WALL',TRANSPARENCY=0 /
72 &OBST XB=1.4,4.55,3.09,3.21,0,5.5,SURF_ID='WALL',TRANSPARENCY=0 /
73 &OBST XB=4.55,4.66,0.73,3.46,0,5.5,SURF_ID='WALL',TRANSPARENCY=0 /
74 &OBST XB=4.55,6.49,1.43,1.55,0,5.5,SURF_ID='WALL',TRANSPARENCY=0 /
75 &OBST XB=5.21,5.32,1.43,3.46,0,5.5,SURF_ID='WALL',TRANSPARENCY=0 /
76 &OBST XB=2.82,2.93,3.46,5.25,0,5.5,SURF_ID='WALL',TRANSPARENCY=0 /
77 &OBST XB=4.67,4.78,3.46,5.25,0,5.5,SURF_ID='WALL',TRANSPARENCY=0 /
78

79 &HOLE XB=1.84,2.39,5.25,5.37,0,2 /
80 &HOLE XB=3.53,4.1,5.25,5.37,0,2 /
81 &HOLE XB=6.47,6.58,4.08,4.63,0,2 /
82 &HOLE XB=4.67,4.78,3.95,4.76,0,2 /
83 &HOLE XB=0.61,0.72,1.455,2.265,0,2 /
84 &HOLE XB=0.61,0.72,3.715,4.525,0,2 /
85 &HOLE XB=6.47,6.58,2.1,2.91,0,2 /
86 &HOLE XB=4.66,5.21,1.43,1.55,0,2 /
87 &HOLE XB=4.66,5.21,3.46,3.58,0,2 /

```

88 &HOLE XB=4.55,4.66,0.85,1.43,0,2/
89 &HOLE XB=1.6,2.41,3.09,3.21,0,2/
90 &HOLE XB=5.5,6.31,0.73,0.85,0,2/
91
92
93
94 &SURF ID='SUPPLY',VEL=-1.75 /
95 &VENT XB=0.2,0.3,1.22,4.78,0,0,SURF_ID='SUPPLY',COLOR='CYAN' /
96 &SURF ID='SUPPLY',VEL=-1.75 /
97 &VENT XB=2.72,6.28,0.2,0.3,0,0,SURF_ID='SUPPLY',COLOR='CYAN' /
98 &SURF ID='SUPPLY',VEL=-1.75 /
99 &VENT XB=8.6,8.8,1.22,4.78,0,0,SURF_ID='SUPPLY',COLOR='CYAN' /
100 &SURF ID='SUPPLY',VEL=-1.75 /
101 &VENT XB=2.72,6.28,5.6,5.8,0,0,SURF_ID='SUPPLY',COLOR='CYAN' /
102
103
104
105 &MULT ID='VENTS',DX=1,DY=1.2,ILOWER=1,IUPPER=8,JLOWER=1,JUPPER=4/
106 &HOLE XB=0,0.15,0,0.15,5.4,5.576,MULT_ID='VENTS',COLOR='RED' /
107 &OBST XB=0,9,0,6,5.9,6,SURF_ID='WALL',OUTLINE=.TRUE. /
108 &SURF ID='OUTLET',VOLUMEFLOW=3,COLOR='RED' /
109 &VENT XB=0,9,0,6,5.9,5.9,SURF_ID='OUTLET' /
110
111 &OBST XB=-0.1,0,0,6,5,6,SURF_ID='WALL' /
112
113
114
115 &VENT MB='XMIN',SURF_ID='OPEN' /
116
117 &SLCF PBX=7.17,'QUANTITY="TEMPERATURE" _/

```

118 &SLCF_PBX=7.17, 'QUANTITY="HRRPUV" /
119 &SLCF_PBX=7.17, 'QUANTITY="MIXTURE_FRACTION" /
120 &SLCF_PBX=7.17, 'QUANTITY="TEMPERATURE" , VECTOR=.TRUE. /
121 &SLCF_PBY=3.09, 'QUANTITY="TEMPERATURE" , VECTOR=.TRUE. /
122 &SLCF_PBZ=2.2, 'QUANTITY="TEMPERATURE" , VECTOR=.TRUE. /
123 &SLCF_PBX=7.17, 'QUANTITY="TEMPERATURE" , VECTOR=.TRUE. /
124 &SLCF_PBZ=1.9, 'QUANTITY="TEMPERATURE" , VECTOR=.TRUE. /
125 &SLCF_PBZ=5.7, 'QUANTITY="TEMPERATURE" , VECTOR=.TRUE. /
126
127
128
129 &TAIL /

Bibliography

- [1] W.K. Chow, and K.W. Lau, *Field tests on atrium smoke control systems.*, ASHRAE Transactions (1995): 101(1):461-469.
- [2] L.Y. Cooper, *Heat transfer from a buoyant plume to an unconfined ceiling.*, ASME Journal of Heat Transfer (1982): 104: 446.
- [3] J.W. Deardorff., *Stratocumulus-capped mixed layers derived from a three-dimensional model.*, Boundary-Layer Meteorol, (1980): 18:495-527.
- [4] U.S. Fire Administration, *U.S. fires deaths, fire death rates, and risk of dying in a fire.*, USFA. 27 August 2018 https://www.usfa.fema.gov/data/statistics/fire_death_rates.html
- [5] Z. Fu, and G. Hadjisophocleous, *A two-zone fire growth and smoke movement model for multi-compartment buildings.*, Fire Safety Journal (2000): 34: 257.
- [6] G. Hadjisophocleous, Z. Fu, G. Lougheed, *A computational and experimental study of smoke movement in a 10-storey building using a two-zone model.*, In: InterFlam, 9th International Fire Science and Engineering Conference, Edinburgh; Scotland, (2001): pp. 1047-1058.
- [7] G. Heskestad, *Fire Plumes.*, The SFPE Handbook of Fire Protection Engineering, Quincy, Mass.: National Fire Protection Association (1995): p. 2-9.
- [8] J.P. Holman, *Heat Transfer.*, McGraw-Hill, New York, 7th Edition (1990).
- [9] N. Jarrin, *Synthetic Inflow Boundary Conditions for the Numerical Simulation of Turbulence.*, University of Manchester, Manchester M60 1QD, United Kingdom (2008).
- [10] B.J. McCaffrey, *Momentum implications for buoyant diffusion flames.*, Combustion and Flame (1983): 52:149.
- [11] K. McGrattan, S. Hostikka, R. McDermott, J. Floyd, M. Vanella, C. Weinschenk, and K. Overholt, *Fire Dynamics Simulator User's Guide 6th Edition*, National Institute of Standards and Technology, 1 November 2017
- [12] K. McGrattan, S. Hostikka, R. McDermott, J. Floyd, M. Vanella, *Fire Dynamic Simulator Technical Reference Guide Volume1: Mathematical Model 6th Edition*, National Institute of Standards and Technology, 26 June 2017
- [13] J. H. McGuire, *Smoke Movement in Buildings*, Fire Technology, (1967) 3:163
- [14] F. Nicoud and F. Ducros, *Subgrid-Scale Stress Modelling Based on the Square of the Velocity Gradient Tensor.*, Flow, Turbulence, and Combustion (1999): 62:183-200.

- [15] J. Smagorinsky., *General Circulation Experiments with the Primitive Equations I. The Basic Experiment.*, Monthly Weather Review (1963): 91(3):99-164.
- [16] B. Vreman., *An eddy-viscosity subgrid-scale model for turbulent shear flow: Algebraic theory and applications.*, Physics of Fluids (2004): 16(10):3670-3681.
- [17] Y. Wang, G. Hadjisophocleous, E. Zalok, *Smoke movement in multi-storey buildings using CUsmoke.*, Safety Science (2012): 52 (2013) 13-27.
- [18] Wikipedia Contributors, *Flashover*, Wikipedia, The Free Encyclopedia. 24 July, 2018. <https://en.wikipedia.org/w/index.php?title=Special:CiteThisPage&page=Flashover&id=851794800>
- [19] Wikipedia Contributors, *Smoke Inhalation.*, Wikipedia, The Free Encyclopedia. 7 May 2018. https://en.wikipedia.org/w/index.php?title=Smoke_inhalation&oldid=840070279
- [20] D.C. Wilcox, *Turbulence Modeling for CFD.*, DCW Industries, Inc., 2nd edition (1998).

Date: September 2018

Curriculum Vitae

Robin Wu, M.S.

4505 South Maryland Parkway
College of Engineering
University of Nevada, Las Vegas
Las Vegas, NV, 89154-4005
Phone: (702)-895-3699
Email: wur1@unlv.nevada.edu

Education

University of Alabama, Tuscaloosa
B.S., Engineering, May 2012

University of Nevada, Las Vegas
M.S., Engineering, December 2018